# Observations of speciated isoprene nitrates in Beijing: implications for isoprene chemistry

Claire E. Reeves[1], Graham P. Mills[1], Lisa K. Whalley[2], W. Joe F. Acton[3], William J. Bloss[4], Leigh R. Crilley[4,5], Sue Grimmond[6], Dwayne E. Heard[7], C. Nicholas Hewitt[3], James R. Hopkins[8], Simone Kotthaus[6,9], Louisa J. Kramer[4], Roderic L. Jones[10], James D. Lee[8], Yanhui Liu[1], Bin Ouyang[10], Eloise Slater[7], Freya Squires[11], Xinming Wang[12], Robert Woodward-Massey[13], and Chunxiang Ye[13]

[1]Centre for Ocean and Atmospheric Sciences, School of Environmental Sciences, University of East Anglia, UK
[2]National Centre for Atmospheric Science, School of Chemistry, University of Leeds, UK
[3]Lancaster Environment Centre, Lancaster University, Lancaster, UK
[4]School of Geography, Earth and Environmental Sciences, the University of Birmingham, Birmingham, B15 2TT, UK
[5]now at Department of Chemistry, York University, Toronto, Canada.
[6]Department of Meteorology, University of Reading, Reading, UK
[7]School of Chemistry, University of Leeds, UK
[8]National Centre for Atmospheric Science, Wolfson Atmospheric Chemistry Laboratories, Department of Chemistry, University of York, UK
[9]Institut Pierre Simon Laplace, Ecole Polytechnique, France
[10]Department of Chemistry, University of Cambridge, UK
[11]Wolfson Atmospheric Chemistry Laboratories, Department of Chemistry, University of York, UK
[12]Guangzhou Institute of Geochemistry, Chinese Academy of Sciences, Guangzhou, China
[13]Beijing Innovation Center for Engineering Science and Advanced Technology, State Key Joint Laboratory for Environmental Simulation and Pollution Control, Center for Environment and Health, College of Environmental Sciences and Engineering, Peking University, Beijing, 100871, China

*Correspondence to*: Claire E. Reeves (c.reeves@uea.ac.uk)

**Abstract.** Isoprene is the most important biogenic volatile organic compound in the atmosphere. Its calculated impact on ozone ($O_3$) is critically dependent on the model isoprene oxidation chemical scheme, in particular the way the isoprene-derived organic nitrates (IN) are treated. By combining gas chromatography with mass spectrometry, we have developed a system capable of separating, and unambiguously measuring, individual IN isomers. In this paper we use measurements from its first field deployment, which took place in Beijing as part of the Atmospheric Pollution and Human Health in a Chinese Megacity programme, to test understanding of the isoprene chemistry as simulated in the Master Chemical Mechanism (MCM) (v.3.3.1). Seven individual isoprene nitrates were identified and quantified during the campaign: two β-hydroxy nitrates (IHN); four δ-carbonyl nitrates (ICN); and propanone nitrate.

Our measurements show that in the summertime conditions experienced in Beijing the ratio of (1-OH, 2-$ONO_2$)-IHN to (4-OH, 3-$ONO_2$)-IHN (the numbers indicate the carbon atom in the isoprene chain to which the radical is added) increases at NO mixing ratios below 2 ppb. This provides observational field evidence of the redistribution of the peroxy radicals derived from OH oxidation of isoprene away from the kinetic ratio towards a new thermodynamic equilibrium consistent with box model calculations. The observed amounts of δ-ICN demonstrate the importance of daytime addition of $NO_3$ to isoprene in Beijing but suggest that the predominant source of the δ-ICN in the model (reaction of NO with δ-nitrooxy peroxy radicals) may be too large. Our speciated measurements of the four δ-ICN exhibit a mean C1:C4 isomer ratio of 1.4 and a mean *trans:cis* isomer ratio of 7 and provide insight into the isomeric distribution of the δ-nitrooxy peroxy radicals. Together our measurements and model results indicate that propanone nitrate was formed from the OH oxidation of δ-ICN both during the day and night, as well as from $NO_3$ addition to propene at night.



**Deleted:** report
**Deleted:** (APHH-Beijing)
**Deleted:** .
**Deleted:** summer
**Deleted:** isoprene
**Deleted:** isoprene
**Deleted:** Box model simulations using the Master Chemical Mechanism (MCM) (v.3.3.1) were made to assess the key processes affecting the production and loss of the IN. ¶
**Deleted:** The observed mixing ratios of the two β-IHN are well correlated with an $R^2$ value of 0.85. The mean for their …
**Deleted:** ((
**Deleted:** :
**Deleted:** ) is 3.4
**Deleted:** in the names
**Deleted:** (C)
**Deleted:** ).
**Deleted:** observed ratio tends to increase with decreasing mixing ratios of nitric oxide (NO), although p
**Deleted:** relationship is weak due to there being only a few data points. Examining this relationship in a box model demonstrates that it is largely a reflection…
**Deleted:** respective β-IHN precursor
**Deleted:** which, at NO mixing ratios of less than 1 part per billion (ppb) shift towards those…
**Deleted:** (1-OH, 2-$ONO_2$)-IHN. The
**Deleted:** , however, tends to simulate lower ratios than observed.¶ ¶ Of the δ-ICN, the two *trans* (E) isomers are observed to have the highest mixing ratios and the mean …
**Deleted:** (E-(4-$ONO_2$, 1-CO)-ICN to E-(1-$ONO_2$, 4-CO)-ICN)) is 1.4, which is considerably lower than the expected…
**Deleted:** 6 for addition of $NO_3$ in the C1 and C4 carbon positions in the isoprene chain. The model produces far more δ-ICN than observed, particularly…
**Deleted:** and it also simulates an increase in the daytime δ-ICN that greatly exceeds that seen in the observations. Interestingly, the modelled source of δ-ICN is predominantly during the daytime, due to the presence in Beijing of appreciable daytime amounts of $NO_3$ along with isoprene. δ-ICN is modelled to be the main precursor for propanone nitrate, but their modelled ratio is very different from the observed. The model also simulated large enhancements of (1-OH, 4-$ONO_2$)-IHN and δ-ICN on some nights, but we did not observe these enhancements in δ-ICN and, despite the modelled mixing rations of (1-OH, 4-$ONO_2$)-IHN being above our detection limit, we did not detect it…

This study demonstrates the value of speciated IN measurements in testing understanding of the isoprene degradation chemistry and shows how more extensive measurements would provide greater constraints. It highlights areas of the isoprene chemistry that warrant further study, in particular the impact of NO on the formation of the IHN, and the $NO_3$ initiated isoprene degradation chemistry as well as the need for further laboratory studies on the formation and the losses of IN, in particular via photolysis of δ-ICN and hydrolysis.

## 1 Introduction

Isoprene is the most important biogenic volatile organic compound (BVOC) in the atmosphere, with its emissions accounting for around 500 Tg $yr^{-1}$, about half of the global biogenic non-methane VOC emissions (Guenther et al., 2012). It is emitted by vegetation primarily during the daytime as a function of temperature and solar radiation and is readily oxidised by the hydroxyl (OH) and nitrate ($NO_3$) radicals and ozone ($O_3$). Through its degradation chemistry, isoprene impacts $O_3$ and the formation of secondary organic aerosols (SOA), which together impact the oxidising capacity of the atmosphere and radiative forcing. Global and regional model studies have shown that the calculated impact of isoprene on $O_3$ is critically dependent on the model isoprene oxidation chemical scheme, in particular the way the isoprene-derived nitrates (IN) are treated (e.g. Emmerson and Evans, 2009; Fiore et al., 2005; Squire et al., 2015; von Kuhlman et al., 2004; Wu et al., 2007; Bates and Jacob, 2019; Schwantes et al., 2020). Much of the uncertainty in this chemistry is related to the yield and fate of IN, in particular whether $NO_X$ (nitrogen oxides) and radicals, which are tied up in the nitrates, are later recycled or lost from the atmosphere.

First generation IN are formed following oxidation of isoprene by either OH or $NO_3$ (Wennberg et al., 2018) (Fig. 1). On oxidation by OH, peroxy radicals are formed which when they react with nitric oxide (NO) can lead to the formation of hydroxy nitrates (IHN). These are dominated by β-IHN, but some δ-IHN are also formed. Depending on the fate of the peroxy radicals formed following $NO_3$ addition, a variety of IN can be produced: isoprene hydroperoxy nitrates (IPN); isoprene dinitrates (IDN); isoprene carbonyl nitrates (ICN); as well as IHN. The fate of first generation IN is poorly understood but much advancement in recent years has been made through new laboratory studies following the synthesis of some of the IN (Jacobs et al., 2014; Lee et al., 2014; Lockwood, et al., 2010; Teng et al., 2017; Xiong et al., 2016), but these are still limited to specific IN isomers (six IHN and one ICN) and reaction rate constants for others are based on extrapolation and structural activity relationships. The IN are lost via reaction with OH, $O_3$ and $NO_3$ (Wennberg et al., 2018) and by photolysis (Xiong et al., 2016; Müller et al., 2014) and deposition (Nguyen et al., 2015), and have lifetimes of the order of a few hours. Reactions of the IHN and ICN with OH can lead to the formation of carbonyls and release of $NO_2$ as well as the formation of shorter chained nitrates such as methyl vinyl ketone nitrate, methacrolein nitrate, propanone nitrate (acetone nitrate) and ethanal nitrate, with the ratio between these two pathways differing for specific IN isomers (Wennberg et al., 2018, hereafter referred to as W2018). More details of the chemistry of IN are given in Sect. 1 of the Supplementary Information (Supp. Info.).

In this study we deploy a new gas chromatography (GC) negative ionisation (NI) mass spectrometry (MS) system (Bew et al., 2016; Mills et al., 2016) in the field for the first time. By separating and unambiguously measuring individual IHN and ICN isomers along with propanone nitrate during a field campaign in Beijing, we are then able to test the isoprene chemistry of the MCM using a box model. We examine how the ratios of the IHN, primarily the β-IHN, can provide insight into the peroxy radicals (ISOPOO) derived from the OH oxidation of isoprene and in particular their relationship with NO (left hand side of Fig 1a), and we use data on ICN, IHN and propanone nitrate to provide insight



**Deleted:** to test our

**Deleted:** . Our interpretation is limited by the uncertainties in our measurements and relatively small data set, but and shows how more

**Deleted:** β-

**Deleted:** show

**Deleted:** ), with a yield of around 4-15 % (e.g. Chen et al., 1998; Chuong and Stevens, 2002). These are dominated by β-IHN, but some δ-IHN are also formed. Although $NO_3$ is mostly present at night, isoprene oxidation by $NO_3$ can be important, particularly in the early evening (Brown et al., 2009) and, due to the larger organic nitrate yield of ~65-80 % (Kwan et al., 2012; Perring et al., 2009b, Rollins et al., 2009; Schwantes et al., 2015), can be responsible for a considerable proportion (~40-50 %) of the IN (Horowitz et al., 2007; von Kuhlmann et al., 2004; Paulot et al., 2012; Xie et al., 2013).…

**Moved down [1]:** ¶
The

**Deleted:** fate of first generation IN is poorly understood and until recently understanding was based on theoretical calculations, with most observational constraints based on measurements of either groups of nitrates as totals, or degradation products that come from more than one reaction and precursor species (Giacopelli et al., 2005; Paulot et al., 2009; Rollins et al., 2009).…

**Deleted:** rates

**Deleted:** Müller

**Deleted:** ¶
¶
One of the key issues is whether $NO_X$ and radicals are returned to the system or whether they remain tied up in second generation nitrates. In the case Reactions

**Deleted:** reactions

**Deleted:** or

**Deleted:** ). Critically the β-IHN and δ-IHN have different lifetimes and return different fractions of $NO_2$ (Paulot et al., 2012). As the yields of the IHN from the β and δ peroxy radicals are fairly similar (Teng et al., 2017), a key factor in the amount of $NO_X$ recycled is the relative yields of the β and δ peroxy radicals from OH oxidation of isoprene.¶
¶
Over the last decade or so there has been a considerable effort to improve understanding of isoprene oxidation mechanisms, with the latest understanding detailed in Wennberg et al. (2018) (hereafter referred to as W2018).…

**Deleted:** The implications of this chemistry have been subject to several model studies (Fiore et al., 2005; Wu et al., 2007; Emmerson and Evans, 2009; Paulot et al., 2012; Xie et al, 2013; Squire et al., …

**Deleted:** to separate the IHN (Werner et al., 1999; Giacopelli et al., 2005; Grossenbacher et al., 2001; 2004), but without synthesised …

**Deleted:** mass spectrometry (CIMS) (e.g. Beaver et al., 2012; Xiong et al., 2015; Fisher et al., 2016; Lee et al., 2016; Lee et al., …

**Deleted:** ), we

**Deleted:** 2016), Vasquez et al. (2018) and Li et al. (2019) have developed systems capable of separating, and unambiguously …

**Deleted:** , allowing us to quantify the concentrations of several of the. By

**Deleted:** ,

**Deleted:** major

**Deleted:** as described in Sect. 3. In Sect. 4 we present the observed time series of the measured IN, examine their ratios and diel patter…

**Deleted:** to

**Deleted:** ratio

**Deleted:** isomers and how their ratio changes

**Deleted:** , and to assess the key processes affecting the production and loss of all the IN measured (Sect. 5). …

into the chemistry of the δ-nitrooxy peroxy radicals ($INO_2$) formed from $NO_3$ addition to isoprene and the (right hand side of Fig 1a).

## 2 Nomenclature

In this paper when naming the IN we have followed the nomenclature described by W2018. We assign numbers to the carbons of isoprene based on the conjugated butadiene backbone being comprised of carbons 1−4, with the methyl substituent (carbon 5) connected to carbon 2. We refer to these carbons as "C#" without subscripts (e.g., "C2"). For functionalized isoprene oxidation products, we drop the "C" when describing substituent positions; for example, (1-OH, 2-$ONO_2$)-isoprene hydroxy nitrate (IHN) has a hydroxy group at C1 and a nitrooxy group at C2. This is different to the way we named the IN in Mills et al. (2016) in which the IHN naming followed that of Lockwood et al. (2010) and the ICN were named similarly to the equivalent IHN, except they have "–al" as a suffix. We referred to acetone nitrate as NOA in Mills et al. (2016) whereas here we refer to it as propanone nitrate.

## 3 Field campaign and measurements

### 3.1 Field campaign overview

The GC-NI-MS system was deployed at the Institute of Atmospheric Physics (IAP, Chinese Academy of Sciences) in the summer of 2017 (21st May to 22nd June) as part of the Atmospheric Pollution and Human Health in a Chinese Megacity (APHH-Beijing) programme (Shi et al., 2019). The IAP is located at 39.97° N, 116.38° E in a residential area between the 3rd and 4th North ring roads of Beijing. The site contained small trees and grass, with roads 150 m away. During the campaign air quality was poor (Fig. S1) with average concentrations of $PM_{2.5}$ of ~30 μg $m^{-3}$ and average mixing ratios of $NO_2$ of 15 ppb, CO of 450 ppb and $O_3$ of ~45 ppb (Shi et al., 2019). Details of the isoprene nitrate measurement technique are provided below, whilst details of instrumentation used for the supporting data are provided in the Supp. Info.

### 3.2 Isoprene nitrate measurement method

Seven individual isoprene nitrates were identified and quantified during the campaign (Figs. 1 and S2): two β-IHN ((1-OH, 2-$ONO_2$)-IHN, (4-OH, 3-$ONO_2$)-IHN); four ICN (E-(1-$ONO_2$, 4-CO)-ICN, Z-(1-$ONO_2$, 4-CO)-ICN, E-(4-$ONO_2$, 1-CO)-ICN, Z-(4-$ONO_2$, 1-CO)-ICN); and propanone nitrate.

Measurements were made approximately hourly. Air was drawn at 10 L $min^{-1}$ down a 2.5 m heated inlet (3/8" PFA and 45 °C) mounted on the roof (a height of approximately 3 m above the ground) of a mobile laboratory. Three different instrument setups were employed: (1) From the start of the measurements to 31 May, samples of 500 ml were taken off the inlet line down a 0.3 m length of 0.53 mm ID MxT-200 transfer line held at 50 °C and preconcentrated on a Tenax adsorption trap at 35 °C and 50 ml $min^{-1}$, and injected onto the column via a metal six port Valco valve by heating to 150 °C (Mills et al. 2016). A 30.5 m, 0.32 mm (internal diameter (ID)) combination column was used which was comprised of 28 m of Rtx-200 followed by 2.5 m of Rtx-1701 column. The GC oven was temperature profiled from 40 °C to 200 °C, with a constant column flow of 4.5 ml $min^{-1}$ of helium; (2) Between 10th June and 16th June, the system was operated without a trap but instead direct injection of a 3 ml sample through a plastic Valco Cheminert valve connected to a short 0.32 mm ID combination column (2.5 m of Rtx-200 joined to 0.5 m of Rtx-1701). The GC oven was temperature programmed from 10 °C to 200 °C and cooled with carbon dioxide ($CO_2$). A constant flow of 6.5 ml

Deleted: Wennberg et al. (2018)

Deleted: campaigns

Deleted: instrumentation

Deleted: campaigns

Deleted: Beijing

Deleted: 2019) during two campaigns at the Institute of Atmospheric Physics (IAP), Chinese Academy of Sciences.…

Deleted: The first campaign was in winter (10th November to 10th December 2016) and the second in the summer (21st May to 22nd June 2017). For reasons discussed below we shall focus on the summer campaign. ¶
¶

Deleted: measurements

Deleted: ¶
This was the first deployment of a GC-NI-MS system in the field to measure speciatedSeven individual

Deleted: .

Deleted: During the summer campaign

min$^{-1}$ of helium was used as the carrier gas; (3) From 18$^{th}$ June to the end, the system again used the 30 m column and Tenax trapping as described above but the metal valve was replaced with the Cheminert valve that was used for the direct injections.

Of the compounds reported here, all but those of (1-OH, 2-$ONO_2$)-IHN and E-(1-$ONO_2$, 4-CO)-ICN were confirmed by injection of known isomers (Mills et al. 2016) post campaign. (1-OH, 2-$ONO_2$)-IHN was identified based on its expected elution just before (4-OH, 3-$ONO_2$)-IHN (Nguyen et al., 2014) and the similarity of the observed ions to those of (4-OH, 3-$ONO_2$)-IHN. The E-(1-$ONO_2$, 4-CO)-ICN peak was identified by its relative elution position compared to the other ICN (Schwantes et al., 2015), its expected retention time estimated from the relative retention times of known δ-IHN on this system and their aldehydic equivalents, and the similarity of observed ions to the other ICN.

During several comparisons of samples measured immediately before and after the valve was changed from metal to plastic and vice versa (1 h between samples), it was evident that the (4-OH, 3-$ONO_2$)-IHN and the ICN were lost to varying degrees on the metal valve as suggested by Crounse (J. D. Crounse, personal communication 2016), while simple alkyl nitrates were not. To account for this, all data obtained with the metal valve were scaled by the ratio of peak areas from the samples on either side of the valve changes to give results equivalent to those obtained when using the Cheminert valve.

Calibrations for (4-OH, 3-$ONO_2$)-IHN and propanone nitrate were derived from the relative sensitivity of the compound to that of n-butyl nitrate (Mills et al., 2016) corrected for the relative ion abundances of the specific measurement ions used for each compound (m/z 71 and 73, respectively). M/z 73 is a relatively minor ion for propanone nitrate, but we were unable to use a more major ion due to interferences from other compounds. N-butyl nitrate calibrations were performed every few days by attaching the transfer line to the standard in place of the inlet. We were unable to measure the relative sensitivities of (1-OH, 2-$ONO_2$)-IHN and the ICNs to n-butyl nitrate directly. To obtain an estimate, we have assumed that the ICN and propanone nitrate all have the same total ion yields compared to those of n-butyl nitrate and scaled this relative total ion yield by the fraction of the ion yield that the measurement ion represents. Similarly we have assumed that the total ion yields of (1-OH, 2-$ONO_2$)-IHN and (4-OH, 3-$ONO_2$)-IHN are the same (and thus the n-butyl nitrate m/z 71: total IN ion ratio) and scaled this to reflect the proportion of the total ions that m/z 101 represents for (1-OH, 2-$ONO_2$)-IHN.

**3.3 Isoprene nitrate measurement uncertainties**

We had previously determined the uncertainty for the measurement of the INs in the laboratory (including the GCMS precision and calibration uncertainties) to be ±14 % (Mill et al, 2016), which includes an uncertainty of 5% for the GCMS precision. For determination of propanone nitrate in the field, we had to use a minor ion, and, with much smaller peaks, the precision was worse than it had been in the laboratory using more abundant ions. Based on the signal to noise on a peak, we estimate that the precision was 10% rather than the 5%. We obtained ion counts per ppt of $NO_Y$ for three isoprene nitrates: (4-OH, 3-$ONO_2$)-IHN (2030), propanone nitrate (2202) Z-(4-OH, 1-$ONO_2$)-IHN (2365). Using this range, we assume an additional uncertainty of 17% for the electron capture / ionisation efficiency of (1-OH, 2-$ONO_2$)-IHN and the ICN. During the campaign, we swapped between a metal and plastic valve twice. Using the peak areas for the last sample with the old valve and first sample with the new valve we calculated loss correction factors as well as the uncertainties in these correction factors of: (4-OH, 3-$ONO_2$)-IHN (±5.2%), propanone nitrate (±6.4%), E-(1-$ONO_2$, 4-CO)-ICN (±14.8%), E-(4-$ONO_2$, 1-CO)-ICN (±9.0%), Z-(1-$ONO_2$, 4-CO)-ICN (±7.5%) and Z-(4-$ONO_2$, 1-CO)-ICN

(±9.2%). Loss corrections were applied to the data collected with the metal valve, and these additional uncertainties included in the overall uncertainties calculated for the periods when the metal valve was used. Based on Mills et al (2016) the detection limit (DL) of our system with the column and trap is 0.1 ppt, but this increased to 1 ppt when run with direct injection. Combining these uncertainties, we get overall uncertainties for the measurements of the IN as shown in Table 1.

When determining the uncertainties in the ratios between IN, we first calculated the uncertainties for each individual IN measurement excluding the calibration uncertainties that were common to both. We then combined the uncertainties in these to derive overall uncertainties in the ratios. We only assessed the ratios of 4-OH, 3-$ONO_2$)-IHN : (1-OH, 2-$ONO_2$)-IHN in period 2, when we the used the plastic valve and direct injection. I.e. for the ratio (4-OH, 3-$ONO_2$)-IHN : (1-OH, 2-$ONO_2$)-IHN, we considered the GCMS precision of 5% for each β-IHN and the additional 17% uncertainty for the electron capture / ionisation efficiency of (1-OH, 2-$ONO_2$)-IHN, plus the 1 ppt for the DL. We only assessed the ICN ratio in period 3 when we the used the plastic valve, along with column and trap. I.e. we considered the GCMS precision of 5% and the additional 17% uncertainty for the electron capture / ionisation efficiency for each of the ICN and 0.1 ppt for the DL.

## 4 MCM Box model set up

A zero dimensional box model, utilising a subset of the chemistry described within the Master Chemical Mechanism, MCMv3.3.1 (Jenkin et al., 2015), was used to calculate the concentrations of the various isoprene nitrates for the campaign. The MCMv3.3.1 includes an update of the isoprene degradation chemistry to reflect findings of recent laboratory and theoretical studies.

The model was constrained by measured values of water vapour, temperature, pressure, NO, $NO_2$, $NO_3$, $O_3$, CO, $SO_2$, HONO and HCHO. Speciated VOC measurements of alcohols, alkanes, alkenes, dialkenes (including isoprene), multi-functional aromatics, carbonyls and monoterpenes were included as further model constraints. The concentrations of $H_2$ and $CH_4$ were held constant at 500 ppb and 1.8 ppm, respectively. The photolysis rates for j($O^1D$), j($NO_2$) and j(HONO), calculated from the measured actinic flux and published absorption cross sections and quantum yields, were included as model inputs. Other photolysis frequencies used in the model were calculated. For UV-active species, such as HCHO and $CH_3CHO$, photolysis rates were calculated by scaling to the ratio of clear-sky j($O^1D$) to observed j($O^1D$) to account for clouds. For species able to photolyse further into the visible the ratio of clear-sky j($NO_2$) to observed j($NO_2$) was used. The variation of the clear-sky photolysis rates ($j$) with solar zenith angle ($\chi$) was calculated within the model using the following expression:

$$j = l\cos(\chi)^m \times e^{-n\sec(\chi)} \quad (3)$$

with the parameters $l$, $m$ and $n$ optimised for each photolysis frequency (see Table 2 in Saunders et al. (2003)).

The model was run for the entirety of the campaign (21st May 2017 – 25th June 2017) in overlapping 7 day segments, with the model constraints updated every 15 minutes. By this method, a model time-series was produced which could be directly compared with observations and, from which, diel averages were generated. There was a spike of very high



**Moved down [2]:** Xiong et al.

**Deleted:** **Field observations**¶
¶
**4.1 Overview of air quality conditions**¶
¶
During the winter campaign air quality was very poor with several haze events and average concentrations of $PM_{2.5}$ of ~90 μg $m^{-3}$, and average mixing ratios of $NO_2$ of 40 ppb, CO of 1300 ppb and $O_3$ of ~8 ppb (Shi et al., 2019). During the summer campaign air quality was also poor, but the mix of pollutants differed, with higher amounts of $O_3$ and lower amounts of $PM_{2.5}$, $NO_2$ and CO. i.e. average concentrations of $PM_{2.5}$ of ~30 μg $m^{-3}$ and average mixing ratios of $NO_2$ of 15 ppb, CO of 450 ppb and $O_3$ of ~45 ppb (Shi et al., 2019). ¶
¶
**4.2 Isoprene nitrate observations**¶
¶
**4.2.1 Time series**¶
¶
The winter campaign was the first field deployment of the GC-NI-MS system for measuring isoprene nitrates. With the very poor air quality the air was loaded with nitrated species which led to many unidentifiable peaks in the chromatograms and, with low temperature and sunlight, biogenic emissions of isoprene were low and no IN were identified. We shall therefore limit our presentation of results to the summer campaign.¶
¶
Seven individual isoprene nitrates were identified and quantified during the summer campaign (Fig. 1): two β-IHN ((1-OH, 2-$ONO_2$)-IHN, (4-OH, 3-$ONO_2$)-IHN); four ICN (E-(1-$ONO_2$, 4-CO)-ICN, Z-(1-$ONO_2$, 4-CO)-ICN, E-(4-$ONO_2$, 1-CO)-ICN, Z-(4-$ONO_2$, 1-CO)-ICN); and propanone nitrate.¶ ...

**Moved down [3]:** (2015) calculate a ratio ranging from 2.6 to 6.0 based on the conditions experienced in SOAS.

**Moved down [4]:** It should be noted that the ratio we obtain from our measurements is not based on an independent calibration for (1-

**Moved down [5]:** ), when we have most confidence in the data (i.e. when the plastic valve was used (Sect. 3.2)), we see that the

**Moved down [6]:** Turning to the E:Z ratios, we observed the E-ICN isomers to dominate over the Z-ICN isomers. The (1-$ONO_2$, 4-

**Moved down [9]:** ). The ratios are higher at night and lower in the daytime. The evening ratios are driven by the preferential

**Moved down [7]:** Fig.

**Moved down [8]:** .¶
¶

**Moved down [10]:** The decrease in this ratio during the morning could be explained if the lifetime of C1-ICN were shorter than for the

**Deleted:** (2015) calculated the sum of the δ-IHN to have made up only a few percent of the total IHN during Southern Oxidant and ...

**Deleted:** Jenkin et al. (2015), using the MCMv3.3.1, calculated that the ratio of (1-OH, 2-$ONO_2$)-IHN to (4-OH, 3-$ONO_2$)-IHN ...

**Deleted:** The β-IHN ratio we obtain is broadly consistent with the studies described above and is examined in more detail with a mo ...

**Deleted:** (2016) for their environmental chamber. In their experiment the ICN mostly came from $RO_2$ + $RO_2$ reactions (see ...

**Deleted:** , as discussed in Sect. S1.1.¶
¶ ...

**Deleted:** 4). This might suggest mixing down of ICN into the mixed layer in the morning but would require considerable ...

**Deleted:** 3

**Deleted:** in Sect. 4.2.2.

**Deleted:** There is a hint of a diel pattern in the ratio of the E and Z isomers of (1-$ONO_2$, 4-CO)-ICN, with larger values at night, but ...

**Deleted:** **modelling**¶
¶ ...

**Deleted:** concentration

**Deleted:** comparison with those measured

concentrations of isoprene in the early hours of the morning of 16th June 2017, which led to extremely high concentrations of modelled ICN, propanone nitrate and (4-OH, 1-$ONO_2$)-IHN. These have been removed from the diel averages presented in this paper. Fluxes through each reaction were calculated for every 15 minute period to allow an analysis of the production and loss terms of the chemical species.

The loss due to mixing of all non-constrained, model generated species, including the speciated isoprene nitrates, was parametrised and evaluated by comparing the model-predicted glyoxal concentration with the observed glyoxal concentration. Applying a loss rate proportional to the observationally-derived mixed layer height (Fig. S4), the model was able to reproduce glyoxal observations reasonably well. As a result of this first order loss process, the partial lifetime of the model generated species was ~2 h at night, then decreased rapidly to a lifetime of <30 min in the morning as the mixed layer grew, effectively simulating ventilation of the model box. With the collapse of the mixed layer in the late afternoon the model lifetime with respect to ventilation of glyoxal (and other model generated species) increased. However, the model has a tendency to underestimate glyoxal concentrations between 4 pm and midnight. This underestimation suggests that either the lifetime with respect to ventilation should be even longer or that the model is underestimating oxidation processes that lead to glyoxal production at these times. The same first order loss was applied to all species and no specific assumptions were made about the background concentrations. Consequently, the rate of mixing may be overestimated for longer-lived species with significant background concentrations and conversely underestimated for shorter-lived species.

## 5 Results and Discussion

### 5.1 β-IHN

Figs. 2 and S3 compare the measured and modelled β-IHN. The shaded areas in Fig. 2 represent ±1 s.d. in the data for each hour of the day and illustrate the large day-to-day variability in the mixing ratios of β-IHN. Note that for (1-OH, 2-$ONO_2$)-IHN there are only 6 days of data, hence why the average diel patterns are strongly affected by the day-to-day variability. This is particularly the case for the measurements where three of the hourly bins contain just one measurement, and the rest have between three and eight measurements.

The observed β-IHN exhibit diel patterns that are broadly in agreement with those modelled and consistent with daytime formation from OH oxidation of isoprene and a shift in competition from the reactions of isoprene-derived peroxy radicals (ISOPOO) with NO to reaction with $HO_2$ as mixing ratios of NO decline from an early morning peak (Fig. S4) and those of the peroxy radicals maximise in the mid-afternoon (Whalley et al., 2020). The observed β-IHN peak around midday and these levels are mostly maintained until around sunset when they decline to reach minimum values just after sunrise. This pattern is also broadly similar to that of total IHN observed during the Southern Oxidant and Aerosol Study (SOAS) (Xiong et al., 2015).

The absolute values of the observed (1-OH, 2-$ONO_2$)-IHN daytime mixing ratios are very similar to those modelled (Figs. 2 and S3). On some days, the observed and modelled (4-OH, 3-$ONO_2$)-IHN mixing ratios are reasonably similar, but on a few days the model simulates considerably larger mixing ratios than observed (Fig. S3) such that the mean daytime observed mixing ratios tend to be lower than modelled and exhibit far less day-to-day variability (Fig. 2). The observed evening mixing ratios of both β-IHN are higher than modelled suggesting that, like glyoxal, the model overestimates their loss with respect to ventilation. Alternatively, there may be greater production or slower chemical

Deleted: 4

Deleted: .2

Deleted: S3

Deleted: 5

Deleted: 5

Moved (insertion) [1]

Deleted: MCM simulates (

Deleted: observed. The modelled

Deleted: lower

Deleted: observed.

Deleted: this underestimation suggests the lifetime

Deleted: might be longer than 2 hours

loss than simulated. It is worth noting that the MCM assumes 8% of the OH addition to isoprene occurs at the C2 and C3 positions instead of the C1 and C4 positions so reducing the potential to form (1-OH, 2-$ONO_2$)-IHN or (4-OH, 3-$ONO_2$)-IHN, whereas W2018 recommend that the C2 and C3 addition are negligible.

To limit the impact of ventilation on the comparison between the model and observations, Figs. 3 and 4 compare the ratios of (1-OH, 2-$ONO_2$)-IHN to (4-OH, 3-$ONO_2$)-IHN. When looking at the times series (Fig. 3) of this ratio the model and measurements often agree within the measurement uncertainties, although there are times when the observed values are greater than modelled. The shaded areas in Fig. 4 represent ±1 s.d. in the data for each hour of the day. The large variability in the observed data is caused by some hours having very few data points, sometimes affected by a single high value (Fig. 3). The observed mean ratios are generally higher than the modelled mean, although there is often agreement within the day-to-day variability.

It should be noted that the ratio we obtain from our measurements is not based on an independent calibration for (1-OH, 2-$ONO_2$)-IHN, but based on the assumption that the analytical system has the same sensitivity to (1-OH, 2-$ONO_2$)-IHN as it does to (4-OH, 3-$ONO_2$)-IHN. We have tried to account for this in the uncertainty calculations by assuming that the error in this sensitivity is equal to the percentage range of sensitivities that we observed for the other IN (see section 3.3). It is possible that this is an underestimate.

There are four main factors that determine the ratio of the β-IHN: 1) the yields of their respective peroxy radicals (ISOPOO) following oxidation of isoprene by OH addition (φ); 2) the fraction of the respective ISOPOO that reacts with NO (γ); 3) the branching ratios for the formation of the IHN from the reaction of NO with the ISOPOO (α); and 4) the relative loss rates of the β-IHN, including via deposition.

For the first two factors, the concentration of NO is largely the determining influence. The adducts formed from OH addition to a specific C in isoprene can form a β-ISOPOO and either an E or Z δ-ISOPOO on reaction with $O_2$ (Fig. 5). These reactions are reversible and, since the lifetimes of these peroxy radicals differ, they interconvert within two subgroups defined by the position of the OH (i.e. C1 on the left hand side of Fig. 5 and C4 on the right hand side). NO is often present in large amounts (Figs S2 and S4) so reaction with it is the dominant loss process for the ISOPOO. However, at low NO mixing ratios, other losses of the ISOPOO become relatively more important and, in particular, the different rates of 1,6 H atom shift isomerisation of the Z-(1-OH, 4-OO)-ISOPOO and Z-(4-OH, 1-OO)-ISOPOO means that redistribution of the ISOPOO within each sub-group differ such that (1-OH, 2-OO)-ISOPOO increases relative to (4-OH, 3-OO)-ISOPOO. Consequently, at lower NO mixing ratios the modelled ratio of φ-(1-OH, 2-OO)-ISOPOO to φ-(4-OH, 3-OO)-ISOPOO becomes larger (Fig. 6a). For mixing ratios of NO greater than ~2 ppb the ratio of the values of φ decreases approximately linearly from around 2 to about 1.7 at 100 ppb of NO. The ratio of the kinetic yields in the MCM is 1.58, which is the ratio of the values of φ that we get if we switch off the reverse pathway of the $O_2$ reactions. This implies that even at 100 ppb of NO, the ratio of the yields of the (1-OH, 2-OO)-ISOPOO to (4-OH, 3-OO)-ISOPOO is shifted to values slightly greater than the kinetic ratio. At NO mixing ratios less than ~2 ppb the ratio of the values of φ increase with decreasing NO, such that at a few 10s of ppt of NO the ratio is typically between 2.5 and 4.

The rates at which the ISOPOO are assumed to be lost via the reactions with NO, $HO_2$ and $NO_3$ are the same for both β-ISOPOO. However, the rate constants for reaction of (1-OH, 2-OO)-ISOPOO with $RO_2$ and for its rate of isomerisation

**Deleted:** During the daytime the (4-OH, 3-$ONO_2$)-IHN modelled by the MCM tends to give larger mean mixing ratios and greater day-to-day variability than observed. This is partially the result of a few days when the model calculates high mixing ratios of (4-OH, 3-$ONO_2$)-IHN that are not observed (Fig. S3). Like the modelled (1-OH, 2-$ONO_2$)-IHN, the concentrations of (4-OH, 3-$ONO_2$)-IHN decline more rapidly in the evening than observed, suggesting that its lifetime with respect to ventilation might be longer than 2 hours. ¶ ¶

**Deleted:** mixing

**Deleted:** ,

**Deleted:** 2

**Deleted:** 6

**Deleted:** 2

**Deleted:** modelled

**Deleted:** less that observed.

**Deleted:** 6

**Deleted:** are

**Deleted:** 2

**Deleted:** MCM simulates

**Deleted:** that,

**Deleted:** lower

**Deleted:** observed

**Deleted:** they are sometimes within the uncertainty of the measured ratio and…

**Moved (insertion) [4]**

**Deleted:** NO is often present in large amounts (Figs 4 and S2) so that reaction with it is the dominant loss process for the ISOPOO. NO is the major factor determining the lifetime of the ISOPOO and therefore the extent of the redistribution of the ISOPOO from a kinetic ratio towards a thermodynamic equilibrium. The adducts

**Deleted:** a *trans*

**Deleted:** *cis*

**Deleted:** .

**Deleted:** occur

**Deleted:** which along with the rapid

**Deleted:** -δ-

**Deleted:** the longer the lifetime

**Deleted:** the more the ratio of the β-ISOPOO shifts towards

**Deleted:** .

**Deleted:** ratio of φ-(1-OH, 2-$ONO_2$)-IHN to φ-(4-OH, 3-$ONO_2$)-IHN becomes larger. This is illustrated in Fig. 7a, which shows the

**Deleted:** the values of φ.

**Deleted:** greatly

**Deleted:** of

**Deleted:** for

are slower than those of (4-OH, 3-OO)-ISOPOO. At lower NO mixing ratios, these reactions become relatively more important and so the modelled value of γ is lower for (4-OH, 3-OO)-ISOPOO than for (1-OH, 2-OO)-ISOPOO, and the ratio of γ-(1-OH, 2-OO)-ISOPOO to γ-(4-OH, 3-OO)-ISOPOO is larger (Fig. 6b). This is further enhanced as the concentrations of $RO_2$ can also be much greater at the lower NO concentrations, particularly below 1 ppb of NO (Fig. 6c), which leads to the ratio in the γ values being considerably greater than 1 at NO concentrations below a few 10s of ppt.

It should be noted that the MCM model underestimates the measured $RO_2$ mixing ratios (Whalley et al., 2020). This will lead to underestimation of the ratio of γ-(1-OH, 2-OO)-ISOPOO to γ-(4-OH, 3-OO)-ISOPOO, primarily at mixing ratios of NO below ~2 ppb. This might explain some of the differences between the MCM modelled and observed β-IHN ratios.

The net effect of these relationships is that the modelled ratio of (1-OH, 2-OO)-ISOPOO to (4-OH, 3-OO)-ISOPOO increases with decreasing NO (Fig. 6d), i.e. for NO mixing ratios greater than 2 ppb the ratio is around 1.7-2.0, but at NO mixing ratios less than 2 ppb the ratio increases up towards a value of around 4. The ratio of the rate of production of (1-OH, 2-$ONO_2$)-IHN to (4-OH, 3-$ONO_2$)-IHN will have the same relationship with NO as the ratio of their precursor ISOPOO since the MCM assumes that the branching ratios for the formation of the two β-IHN from the reaction of NO with the ISOPOO (i.e. α, third factor) are the same. However, there are still considerable uncertainties in these branching ratios (Sect. S1.1).

As for the loss processes of the β-IHN (fourth factor), the dominant loss in the model is the mixing term which is set at the same rate for both β-IHN. Photolysis is assumed to be faster for (1-OH, 2-$ONO_2$)-IHN than for (4-OH, 3-$ONO_2$)-IHN in the MCM, but is only a minor loss process. However, (1-OH, 2-$ONO_2$)-IHN reacts with both OH and $O_3$ more slowly than does (4-OH, 3-$ONO_2$)-IHN and since the dominant chemical loss process for the β-IHN are by far their reactions with OH, the net effect of these loss processes is to increase the ratio of (1-OH, 2-$ONO_2$)-IHN to (4-OH, 3-$ONO_2$)-IHN above their production ratio. The diel pattern in OH (Fig. S4) will tend to increase the ratio of (1-OH, 2-$ONO_2$)-IHN to (4-OH, 3-$ONO_2$)-IHN during the daytime.

Overall, this means that the modelled ratio of (1-OH, 2-$ONO_2$)-IHN to (4-OH, 3-$ONO_2$)-IHN increases with decreasing NO mixing ratios (Fig. 6e) (as also seen by Jenkin et al. (2015) in a box model using the MCM), and generally does not drop below the ratio of the β-ISOPOO (Fig. 6d). In the conditions modelled for Beijing it ranges from between 1.75 and 2.0 at NO mixing ratios above ~30 ppb rising up to typically between 2 and 3, but sometimes up to 4 at NO mixing ratios below 1 ppb. There are several cases at these low NO mixing ratios when the ratio of the β-IHN is below the ratio of the β-ISOPOO, but these occur at night when the production rates and the mixing ratios of the β-IHN are very small.

In comparison, the observed ratios of (1-OH, 2-$ONO_2$)-IHN to (4-OH, 3-$ONO_2$)-IHN show a similar, but weaker, relationship with NO (Fig. 6f). The strength of the observed relationship is limited by the number of data points and uncertainties in the measurements but shows a tendency for relatively more (1-OH, 2-$ONO_2$)-IHN at NO mixing ratios of less than 1 ppb.

Newland et al., (2020) point out that during the campaign a high $NO_X$ environment existed in the morning but then switched to a low $NO_X$ environment in the afternoon. The mean hourly NO mixing ratios were typically above 2 ppb

Deleted: for

Deleted: therefore

Deleted: 7b

Deleted: 7c

Deleted: .

Deleted: 7d

Deleted: 4

Deleted: ¶
Regarding deposition, it is not included in the MCM model. We expect (1-OH, 2-$ONO_2$)-IHN to be lost more efficiently than (4-OH, 3-$ONO_2$)-IHN given the fast rate of hydrolysis reported for (1-OH, 2-$ONO_2$)-IHN (W2018) (Sect. S1.3.5) and the greater difficulty we have getting (1-OH, 2-$ONO_2$)-IHN through our analytical system indicating a greater loss of this isomer on to surfaces. However, including a greater deposition rate for (1-OH, 2-$ONO_2$)-IHN would reduce the agreement with the observed β-IHN ratios. ¶

Deleted: 7e

Deleted: 7d

Deleted: ,

Deleted: it remains between 1.75 and 2.0. At NO mixing ratios between 1 ppb and ~30 ppb it is mostly around 2.0 but is

Deleted: 3. At NO mixing ratios below 1 ppb, it is

Deleted: that

between 06:00 and 12:00 local time, but mostly below this value in the afternoon (Fig. S4). The relationship between β-IHN and NO as illustrated in (Fig. 6e) largely explains why the modelled ratio of the β-IHN (Fig. 4) is ~2 and exhibits little variability between about 06:00 and 09:00 and then rises up to around 2.5 in the afternoon.

Our mean observed (1-OH, 2-$ONO_2$)-IHN to (4-OH, 3-$ONO_2$)-IHN ratio of ~3.4 is higher than the daytime values reported by Vasquez et al. (2018) in the PROPHET campaign (~2.6) and in Pasadena (~1.4), but their data show a similar pattern to ours in that the ratio is higher in the low $NO_X$ environment of PROPHET compared to the high $NO_X$ environment in Pasadena. We cannot rule out calibration differences affecting this comparison and, like us, Vasquez et al (2018) relied on relative calibrations estimates. Also, differences in the observed β-IHN ratios may be due to the amount and reactivity of the peroxy radicals present in the different studies. However, the ratio of 1.4 observed for Pasadena is lower than the kinetic φ ratios of 1.58 and 1.85 based on MCM and W2018 kinetic yields, respectively. Xiong et al. (2015) calculate a ratio ranging from 2.6 to 6.0 based on the conditions experienced in SOAS.

**5.2 δ-ICN**

The MCM assumes all of the δ-ICN formed can be represented by a single species, (1-$ONO_2$, 4-CO)-ICN, called NC4CHO. We shall therefore compare the sum of the observed δ-ICN with the modelled NC4CHO and then look at the speciation as exhibited in the observations.

Both the observed and modelled total δ-ICN peak at night but the observed was typically less than modelled (Fig. 7 and S5), particularly on occasions at night (Fig. S5). This is also illustrated by the large day-to-day variability in the modelled diel patterns not seen in the observations (Fig. 7). The observed diel patterns in the ICN can be seen more clearly in Figs. 8 and S4 and show maximum values in the early night and minimum values during the daytime

The source of δ-ICN is via the addition of $NO_3$ to isoprene followed by addition of $O_2$. This produces δ-nitrooxy peroxy radicals ($INO_2$) (NISOPO2 in the MCM) and, in the conditions simulated for Beijing, the major loss of $INO_2$ is reaction with NO to form $NO_2$ and a δ-nitrooxy alkoxy radical (NISOPO in the MCM), which then reacts rapidly with $O_2$ to form the δ-ICN. Other production pathways for δ-ICN exist in the MCM, but the reaction of $INO_2$ with NO is by far the dominant source of δ-ICN in our simulations. There are some nights when the model simulates large sources of $INO_2$, but typically the modelled production of $INO_2$ maximises in the mid-afternoon. The model is constrained by the observed concentrations of isoprene and $NO_3$ and in the mid-afternoon the observed isoprene mixing ratios are still high and $NO_3$ is around 2 ppt (Fig. S4).

The dominant loss of δ-ICN in the model is the ventilation term, which is greatest during the daytime when the mixed layer is fully developed. The next most important loss processes for δ-ICN are simulated to be photolysis and reaction with OH, which are also both predominantly daytime losses.

The net effect of the production and loss terms is that the modelled δ-ICN increases during the afternoon and maximises during the night-time and the observed δ-ICN are broadly consistent with this (Fig. 7, S4 and S5). We observed around 1-2 ppt of E-(4-$ONO_2$, 1-CO)-ICN during the daytime and this requires a significant daytime source assuming a lifetime of around 30 minutes with respect to photolysis (based on a value of 4.6 x $10^{-4}$ $s^{-1}$ for a solar zenith angle of 0° (Xiong et al., 2016) and adjusting for latitude, time of year and time of day). This source is consistent with the observed presence of $NO_3$ during the daytime. However, the considerably larger modelled mixing ratios of δ-ICN compared to

**Deleted:** 4) when production rates of the

**Deleted:** were also high. This

**Deleted:** 6),

**Deleted:** The modelled variability in this ratio is very small between 06:00 and 09:00 as the ratio of 2 relates to a wide range of NO mixing ratios (~2-30 ppb) (Fig. 7e).…

**Deleted:** In comparison, the

**Deleted:** ratios of

**Deleted:** show a much weaker relationship with NO (Fig. 7f). This may be due to there being far fewer data points and uncertainties in the measurements. The observed ratios tend to be ratio of

**Deleted:** modelled. At times they drop below the kinetic ratio for φ (but with the uncertainty range of the measurements). Despite far more scatter, including 2 outliers with large uncertainties, there is a tendency for higher values of the observed ratio at NO mixing ratios of less than 1 ppb, as simulated the daytime values reported

**Deleted:** the model.¶
¶

**Deleted:** reported lower daytime values for the ratio of (1-OH, 2-$ONO_2$)-IHN to (4-OH, 3-$ONO_2$)-IHN in …

**Deleted:** ) compared to our observations of ~3.4,

**Deleted:** On average our modelled results are close to the ratios observed in PROPHET. We cannot rule o

**Deleted:** lower than the value of around 1.75 that we calculate for NO mixing ratios of 100 ppb, and furthermore, it is also lower than

**Moved (insertion) [2]**

**Moved (insertion) [3]**

**Deleted:** 3

**Deleted:** ¶
The δ-ICN time series (Fig. S4) shows that the MCM often produces far more δ-ICN than observed, particularly at night. This is further illustrated by the diel patterns (Fig. 8), which shows both higher modelled mixing ratios and greater day-to-day variability at night compared to the observations. Moreover, the model simulates an increase in the daytime δ-ICN that far exceeds that seen in the observations. We are unable to assess the ratios of the different δ-ICN isomers using the model as The MCM assumes all of the

**Deleted:** in the MCM

**Deleted:** nitroxy

**Deleted:** NISOPO2

**Deleted:** nitroxy

**Deleted:** (NC4CHO).

**Deleted:** NC4CHO

**Deleted:** NISOPO

**Deleted:** there are

**Deleted:** NISOPO2

**Deleted:** NISOPO2

**Deleted:** when isoprene

**Deleted:** mean $NO_3$ mixing ratios were observed to be

**Deleted:** 4). Consequently, the production of δ-ICN in the model is mostly during the daytime, despite $NO_3$ usually being considered to be more important at night. Comparison of the modelled and observed mixing ratios of the δ-ICNs suggest that this source might be too fast even during the daytime, despite the model being constrained by observed concentrations of isoprene and $NO_3$.…

**Deleted:** Alternatively, the loss processes could be too slow.

**Deleted:** mixing

**Moved (insertion) [11]**

the observed suggests that the modelled source via $NO_3$ oxidation of isoprene might be too fast, or the loss processes too slow.

The same ventilation process has been applied to all model generated species (Sect. 4). For glyoxal, (1-OH, 2-$ONO_2$)-IHN and (4-OH, 3-$ONO_2$)-IHN, the model tends to overestimate the decrease in concentrations from late afternoon onwards suggesting that the lifetime with respect to ventilation should be longer at these times but increasing the lifetime of δ-ICN would lead to their further overestimation. Applying the same loss term to all model species is of course an approximation, not least because the dilution term depends on the concentration of the species in the diluent air.

The MCM uses a photolysis frequency for δ-ICN based on that measured for propanone nitrate, which is equivalent to 3.16 x $10^{-4}$ $s^{-1}$ for a solar zenith angle of 0°. Xiong et al. (2016) determined a higher rate of 4.6 x $10^{-4}$ $s^{-1}$ for (4-$ONO_2$, 1-CO)-ICN for a solar zenith angle of 0°. Increasing rate of photolysis in the model would not only reduce the daytime increase in δ-ICN but would also reduce the amount of modelled δ-ICN that would persist into the night.

Reaction with OH constitutes a similar size loss for δ-ICN as photolysis in the model. The MCM treats all the δ-ICN as (1-$ONO_2$, 4-CO,)-ICN and uses a rate constant for reaction with OH of 4.16 x $10^{-11}$ $cm^3$ $s^{-1}$. W2018 suggests a lower rate constant for reaction of OH with (1-$ONO_2$, 4-CO)-ICN (3.4 x $10^{-11}$ $cm^3$ $s^{-1}$) but a similar rate for (4-$ONO_2$, 1-CO)-ICN (4.1 x $10^{-11}$ $cm^3$ $s^{-1}$). Therefore, treating the two separately in the model and using the W2018 recommended rate constants would, overall, reduce the loss of δ-ICN with respect to OH, increasing discrepancy with the model.

Night-time losses of δ-ICN are reaction with $O_3$ and $NO_3$. The MCM uses a rate coefficient of 2.4 x $10^{-17}$ $cm^3$ $s^{-1}$ for the reaction of δ-ICN with $O_3$, which is 5 times faster than the value of 4.4 x $10^{-18}$ $cm^3$ $s^{-1}$ recommended by W2018, giving a partial lifetime on the order of 12 hours for an $O_3$ mixing ratio of 40 ppb. On the other hand, the MCM uses a rate constant for the reaction of δ-ICN with $NO_3$ which is 10 times slower than that recommended by W2018, but even so the lifetime of δ-ICN with respect to reaction with $NO_3$ as estimated by W2018 is of the order of 4 days, so this loss pathway would have to be much faster to reduce the modelled night-time δ-ICN close to that observed.

Of the observed δ-ICN, the two *trans* (E) isomers have the highest mixing ratios with E-(1-$ONO_2$, 4-CO)-ICN being the most abundant (Fig. 8 and S2). Focusing on the last four days (three nights) of the campaign (Fig. 8), when we have most confidence in the data (i.e. when the plastic valve was used (Sect. 3.2)), we see that the observed ICN C1:C4 isomer ratio, exhibits a diel cycle with higher values at night (mean of 2.0, standard deviation (s.d.) of 0.3) and an overall mean of 1.4 (s.d. of 0.6). These values are considerably lower than would be expected based solely on the addition of $NO_3$ to isoprene occurring in the C1 and C4 positions in a ratio of 6 (C1:C4) (W2018). Our observed ratios are more comparable to the C1:C4 isomer ratio of 2.8 reported in Schwantes et al. (2016) for their environmental chamber, although in their experiment the ICN mostly came from $RO_2$ + $RO_2$ reactions (see Sect. S1.2) because the NO and $NO_3$ concentrations were low. Turning to the E:Z ratios, we observed the E-ICN isomers to dominate over the Z-ICN isomers. The (1-$ONO_2$, 4-CO)-ICN isomers exhibit a mean night-time E:Z ratio of 8 (s.d. of 1.4), whilst the (4-$ONO_2$, 1-CO)-ICN isomers exhibit a mean night-time E:Z ratio of 11 (s.d. of 1.5), giving an overall mean night-time E:Z ratio of 9 (s.d. of 1.0). These values are far greater than the *trans*:*cis* ratio of 1 presumed by W2018 for the reaction of $NO_3$ addition to isoprene, based on the OH addition to C1 of isoprene calculated by Peeters et al. (2009). However, it

**Deleted:** loss
**Deleted:** 5.1
**Deleted:** mixing
**Deleted:** .
**Deleted:** all the model intermediates
**Deleted:** a
**Deleted:** of δ-ICN
**Moved up [11]:** The next most important loss processes for δ-ICN are simulated to be photolysis and reaction with OH, which are also both predominantly daytime losses. The net effect of the production
**Deleted:** The net effect of the production and loss terms is that the modelled δ-ICN maximise during the night-time as obsdeved (Fig. 8).¶ ¶
**Deleted:** Reaction with OH constitutes a similar size loss for δ-ICN asIncreasing rate
**Deleted:** . Whilst these are both predominantly daytime sinks, increasing them
**Deleted:** coefficient
**Deleted:** 1
**Deleted:** However,
**Deleted:** coefficient
**Deleted:** 4
**Deleted:** 1
**Deleted:** than for (1-$ONO_2$, 4-CO,)-ICN
**Deleted:** versus
**Deleted:** rate
**Deleted:** the rate
**Deleted:** to
**Moved (insertion) [5]**
**Moved (insertion) [6]**

should be noted that the peroxy radicals formed from the reaction of the adducts with $O_2$ may be in a different ratio as these reactions are reversible, similar to those for peroxy radicals formed following OH addition to isoprene.

As noted above, the ratios of C1-ICN to C4-ICN ratios exhibit diel patterns (Fig. 8). The ratios are higher at night and lower in the daytime. The evening ratios are driven by the preferential addition of $NO_3$ to the C1 position as discussed above. The decrease in this ratio during the morning could be explained if the lifetime of C1-ICN were shorter than for the other isomers. However, the rate coefficients for reaction with OH recommended by W2018 are about 20 % slower for C1-ICN than for C4-ICN. Photolysis is expected to be the largest daytime sink, but Xiong et al (2016) only determined this for E-(4-$ONO_2$, 1-CO)-ICN.

**5.3 Propanone nitrate**

Figures S5 and 7 show the time series and diel patterns of the measured and modelled propanone nitrate. The observed mixing ratios are generally higher than the modelled values. The chemical lifetime of propanone nitrate is calculated to be around 10 hours during the daytime and considerably longer at night, so transport is expected to play an important role in the distribution of propanone nitrate. The mixing term dominates the modelled lifetime and the resulting mixing ratios are highly dependent on the assumptions regarding this term. As discussed in Section 4, the same first order mixing loss rate is used for all species. As significant concentrations of propanone nitrate are expected to remain in the residual layer, this may lead to an overestimation of the mixing, but reducing this would worsen the comparison with the observed propanone nitrate. Despite these issues the model can still provide insight into the dominant chemical production processes.

The primary source of propanone nitrate in the model is the OH oxidation of δ-ICN, which is formed from $NO_3$ oxidation of isoprene. Consequently, the modelled propanone nitrate and δ-ICN time series share many similarities (Fig. S5). As discussed above, the production of δ-ICN and its loss via OH oxidation occur mostly during the daytime, so this source of propanone nitrate is predominantly during the daytime. On nights when OH is present even at low concentrations it can be a sizeable source due to the relatively large amounts of δ-ICN at night. Propanone nitrate is also formed from oxidation of δ-ICN by $O_3$. This is a relatively small source except on nights when $O_3$ was present (Fig. S1). Propanone nitrate can also be produced following the $NO_3$ addition to propene. Overall, the model results suggest this to be a relatively small source, but is often calculated to be the dominant source of some of the night-time peaks in propanone nitrate.

Both the modelled and observed propanone nitrate reflect the fact that production of propane nitrate can occur both during the daytime and at night (Figs. S5 and 8). Fig. 8 shows the temporal variation of the observed propanone nitrate, along with (4-$ONO_2$, 1-CO)-ICN for the last four days of the campaign. Propanone nitrate exhibits three peaks: two on the nights of the 19-20/06/2017 and 20-21/06/2017, and one during the daytime on the 21/06/2017. These peaks are replicated, but to a lesser extent by the model, which suggests that the peak on the night of the 19-20/06/2017 was OH oxidation of δ-ICN and, to a lesser extent, $NO_3$ addition to propene. The next night $NO_3$ addition to propene was modelled to be the dominant source of the propanone nitrate with OH oxidation of δ-ICN being the main source during the following day. The consequence of this pattern in sources is that both the observed and modelled mixing ratios show no clear diel cycle, possibly a weak bimodal pattern in the mean, and large day-to-day variability (Fig. 7).

**Moved (insertion) [8]**

**Moved (insertion) [9]**

**Moved (insertion) [10]**

**Deleted:** 4

**Deleted:** S4

**Deleted:** 8

**Deleted:** As discussed above, elevated

**Deleted:** mixing ratios are observed both during the daytime and night-time, leading to a weak bimodal pattern in the mean, but there is large day-to-day variability. This is consistent with both daytime and night-time production processes. It should be noted that transport will play an important role in the variability of the propanone nitrate. Its chemical lifetime …

**Deleted:** .

**Deleted:** so

**Deleted:** However,

**Deleted:** The main source of propanone nitrate is via oxidation of isoprene, with routes via both OH and $NO_3$ addition to isoprene. Its…

**Deleted:** MCM simulation

**Deleted:** via the OH

**Deleted:** NC4CHO (i.e. the δ-ICN) and this is reflected in them sharing many similarities in their isoprene.

**Deleted:** S4

**Deleted:** in Sect. 5.3

**Deleted:** NC4CHO

**Deleted:** NC4CHO

**Deleted:** NC4CHO

**Deleted:** S2).¶
¶
The modelled ratio propanone nitrate to δ-ICN is mostly much less than one. Conversely the measured propanone nitrate is typically a lot greater than the total δ-ICN observed. This might, in part be due to the model being unable to simulate the mixing correctly, but, as discussed in Sect. 5.3, the model simulates considerably larger amounts of NC4CHO than observed and getting the wrong balance between the various production and loss terms of NC4CHO (i.e. the δ-ICN) will likely impact the modelled propanone nitrate. ¶
¶

**Deleted:** at night it

**Deleted:** , which may explain

**Moved (insertion) [7]**

**Deleted:** 5.5 δ-IHN¶
¶
The MCM simulates daytime

**Deleted:** for the

The modelled propanone nitrate is generally less than the δ-ICN. In contrast the observed propanone nitrate is typically a lot greater than total δ-ICN. This might, in part be due to the model being unable to simulate the mixing correctly, but, as discussed in Sect. 5.2, the model simulates considerably larger amounts of δ-ICN than observed and getting the wrong balance between the various production and loss terms of the δ-ICN will likely impact the modelled propanone nitrate.

### 5.4 δ-IHN

Four δ-IHN can be formed from the OH addition to isoprene in the C1 and C4 positions: E-(1-OH, 4-$ONO_2$)-IHN, Z-(1-OH, 4-$ONO_2$)-IHN, E-(4-OH, 1-$ONO_2$)-IHN) and Z-(4-OH, 1-$ONO_2$)-IHN) (Fig. 5). The MCM treats the *trans* and *cis* δ-IHN isomers as a single species and so considers two δ-IHN: (1-OH, 4-$ONO_2$)-IHN and (4-OH, 1-$ONO_2$)-IHN. The modelled two δ-IHN are simulated to have very similar mixing ratios during the daytime, with peaks values of around 1 ppt (Figs. 9 and S6). Whilst we have previously demonstrated that our system can measure the four δ-IHN (Mills et al., 2016) we found no evidence of them in Beijing despite the modelled daytime mixing ratios being above our detection limit of 0.1 ppt.

The model also simulates enhancements of (4-OH, 1-$ONO_2$)-IHN of around 15-30 ppt on several nights coincident with enhanced mixing ratios of the δ-ICN (Figs. 9 and S6), because (4-OH, 1-$ONO_2$)-IHN is also formed when the $INO_2$ radicals react with organic peroxy radicals. As discussed in Sect. 5.2, $INO_2$ is mostly produced during the daytime, but on some nights $INO_2$ mixing ratios were simulated to be high leading to these elevated mixing ratios of both (4-OH, 1-$ONO_2$)-IHN and δ-ICN. We were only making measurements on a few of the nights when the model simulates these enhancements in (4-OH, 1-$ONO_2$)-IHN, but again we did not detect it and although we saw small enhancements in δ-ICN they were far smaller than modelled.

## 6 Conclusions

Following OH oxidation of isoprene, the concentration of NO is critical in determining the lifetime, fate and redistribution of the isoprene-derived peroxy radicals, ISOPOO. Measuring IHN, products of the reactions between NO and ISOPOO, provide observational insight into this chemistry. Our measurements show that in the summertime conditions experienced in Beijing the β-IHN ratio ((1-OH, 2-$ONO_2$)-IHN to (4-OH, 3-$ONO_2$)-IHN) increases at NO mixing ratios below 2 ppb providing observational field evidence of the redistribution of the ISOPOO away from the kinetic ratio towards a new thermodynamic equilibrium consistent with box model calculations.

There are absolute discrepancies between the modelled and observed ratio of β-IHN, with the observed values being higher. Some of this might be resolved with a more accurate calibration of (1-OH, 2-$ONO_2$)-IHN. However, there may be issues with the chemical scheme and it is noteworthy that the model underestimates the measured $RO_2$ mixing ratios, for both those classed as simple and those as complex, the latter which include ISOPOO (Whalley et al., 2020). Whilst an underestimation of the β-ISOPOO might impact the absolute mixing ratios of modelled β-IHN, an underestimation of the total $RO_2$ can affect the β-IHN ratio as the rate constant for the reaction of $RO_2$ with (1-OH, 2-OO)-ISOPOO is slower than that for reaction of $RO_2$ with (4-OH, 3-OO)-ISOPOO and this contributes to the higher β-IHN ratios at the lower NO mixing ratios.

**Deleted:** (i.e. (1-OH, 4-$ONO_2$)-IHN and (4-OH, 1-$ONO_2$)-IHN), consistent with production can be formed

**Deleted:** , of around 1 ppt (Figs. 9 and S5). As mentioned above, we were unable to detect these IN in Beijing despite having been able to in the laboratory. The in the C

**Deleted:** , but on several nights,

**Deleted:** are simulated and these are

**Deleted:** modelled

**Deleted:** . As well as being formed by OH oxidation of isoprene,

**Deleted:** in the MCM

**Deleted:** NISOPO2

**Deleted:** produced by $NO_3$ oxidation of isoprene

**Deleted:** other

**Deleted:** above

**Deleted:** 3, NISOPO2 are

**Deleted:** present

**Deleted:** NISOPO2

**Deleted:** Only

**Deleted:** simulated night-time peaks occurred at times

**Deleted:** we were making measurements, but despite the modelled mixing ratios of around 15-30 ppt being well above our detection limit we did not to detect (4-OH, 1-$ONO_2$)-IHN. Also, despite successfully measuring the δ-ICN, we did not detect strong the model

**Deleted:** their mixing ratios

**Deleted:** ¶
Examining the ratio of the two β-IHN in a box model demonstrates its sensitivity to NO, which affects the thermodynamic equilibrium of the β-ISOPOO and the competition between the reactions of the β-ISOPOO with NO and with $RO_2$. In both cases, lower NO mixing ratios favour (1-OH, 2-$ONO_2$)-IHN over (4-OH, 3-$ONO_2$)-IHN. Interestingly, in high $NO_X$ conditions the modelled β-IHN ratio ((1-OH, 2-OO)-ISOPOO to (4-OH, 3-OO)-ISOPOO) of around 2 exceeds the kinetic ratio. At NO mixing ratios below 2 ppb the competition between the reactions of the β-ISOPOO with NO and with $RO_2$ become important and this results in modelled β-IHN ratios greater than 2, approaching 4 for NO mixing ratios of a few 10s of ppt. ¶
¶
The observed mean β-IHN ratio is 3.4, higher than modelled. The relationship of the observed β-IHN ratio with NO is much weaker than modelled, partly due to far fewer data points, but it confirms the theoretical understanding in so far as there tend to be larger ratios at sub 2 ppb amounts of NO.¶
¶
The diel variation in NO mixing ratios means that the $NO_X$ environment observed in Beijing typically switched from a high $NO_X$ environment in the morning to a low $NO_X$ environment in the afternoon resulting in a diel pattern of the modelled β-IHN ratio. However, this is not reflected in the observations, largely due to lack of measurements and the day-to-day variability seen on the few days of available data. More observations of speciated β-IHN and a more accurate calibration of (1-OH, 2-$ONO_2$)-IHN are needed to better constrain these relationships and the underlying chemistry.¶
¶
Of the δ-ICN, the two *trans*

The diel pattern in observed NO (along with OH and peroxy radicals) in Beijing suggests that the ratio of (1-OH, 2-$ONO_2$)-IHN to (4-OH, 3-$ONO_2$)-IHN should have increased during the afternoon, but, unfortunately, we were unable to make enough measurements to observe this given the day-to-day variability in atmospheric composition. However, our observations demonstrate that more extensive measurements of individual β-IHN should provide insight into the β-ISOPOO speciation, and how it changes under different chemical regimes.

Like the β-IHN, δ-IHN are formed following OH addition to isoprene in the C1 and C4 positions and their rates of production are dependent on the kinetic yields of their respective ISOPOO from $O_2$ reaction with the C1 and C4 adducts, and redistribution amongst the ISOPOO. The rapid isomerization of the Z-δ-ISOPOO leads to a greater β:δ ISOPOO ratio than the kinetic one. Whilst the model strongly favours production of β-IHN over the δ-IHN it still suggests that there should be enough δ-IHN present during the daytime for us to detect with our measurement system. However, we found no evidence of their presence, which may suggest that the model underestimates the β:δ ISOPOO ratio, or underestimates the δ-IHN losses.

The observed amounts of δ-ICN demonstrate the importance of daytime addition of $NO_3$ to isoprene in Beijing. Hamilton et al. (2021) have also shown this source of organic nitrates to be important for the formation secondary organic aerosol in Beijing. We did, however, observed far less δ-ICN than we modelled which may suggest that the predominant source of the δ-ICN in the model (reaction of NO with δ-nitrooxy peroxy radicals) is too large or the sink too small. The main source of propanone nitrate in the model is the OH oxidation of δ-ICN so the atmospheric budgets of these two nitrates are linked. Observations of propanone nitrate suggest it can be a marker of this chemistry, although other sources, such as the $NO_3$ addition to propene and the transport of propane nitrate need to be taken into consideration. The model suggests that reaction of the δ-nitrooxy peroxy radicals with organic peroxy radicals is a significant source of (4-OH, 1-$ONO_2$)-IHN at night, but one that is not supported by our observations.

Our speciated measurements of the four δ-ICN isomers provide insight into the isomeric distribution of the δ-nitrooxy peroxy radicals. The two *trans* δ-ICN isomers are observed to have the highest mixing ratios, with E-(1-$ONO_2$, 4-CO)-ICN being the most abundant. However, the mean C1:C4 isomer ratio is 1.4, which is considerably lower than would be expected based solely on the addition of $NO_3$ to isoprene occurring in the C1 and C4 positions in a 6:1 ratio. This raises the question as to whether it is appropriate to represent the δ-ICN by a single C1 nitrated isomer, as done in the MCM. We observed the *trans*-ICN isomers to dominate over the *cis*-ICN isomers with a mean ratio of 7, far greater than the *trans*:*cis* ratio of 1 presumed by W2018 for the reaction of $NO_3$ addition to isoprene. This suggests that thermodynamic redistribution of the δ-nitrooxy peroxy radicals may also be important.

This study demonstrates the value of speciated IN measurements in testing understanding of the isoprene degradation chemistry and more measurements would provide more robust constraints. One reason for the limited data was the need for a different instrument set up for the measurement of (1-OH, 2-$ONO_2$)-IHN. Resolving this would increase data capture and provide concurrent measurements of a range of speciated IN that can be used to test different aspects of the isoprene degradation system simultaneously, including the balance between OH and $NO_3$ oxidation of isoprene. Observations of speciated IN in a wide range of NO/VOC chemical space at different times of day would provide greater constraint on their chemistry, in particular the isomeric distribution and fate of the peroxy radicals. The chemistry of the isoprene degradation chemistry is complex involving multiple species and reactions. Analysis of field measurements of IN can help constrain aspects of this, but interpretation would be enhanced by simultaneous

**Deleted:** nitrated

**Deleted:** formed from the reaction of the $NO_3$-isoprene adducts with $O_2$…

**Deleted:** The observed δ-ICN exhibit nocturnal peaks with maximum values in the early night and minimum values during the daytime are consistent with formation from $NO_3$ addition to isoprene in the evening and a lifetime of the order of a few hours or less. Mixing ratios of 1-2 ppt persist through the daytime, which for the afternoon can be accounted for by the presence of 1-2 ppt of $NO_3$. The model produces far more δ-ICN than observed, particularly at night but it also simulates an increase in the daytime δ-ICN that greatly exceeds that seen in the observations. Reaction of NO with NISOPO2, which comes from $NO_3$ addition to isoprene, is modelled to be by the far the dominant source of δ-ICN. Interestingly, though this source occurs predominantly during the daytime, due to the presence in Beijing of appreciable daytime amounts of $NO_3$ along with isoprene.¶
¶
Observed propanone nitrate shows no clear diel cycle. The pattern can change from day to day, sometimes peaking during the daytime and sometimes at night. The model suggests that the main source of propanone nitrate is the daytime OH oxidation of δ-ICN. However, the model simulates considerably larger amounts of δ-ICN than observed and getting the right balance between the various production and loss terms of δ-ICN is important for modelling the propanone nitrate. Whilst the model results suggest the $NO_3$ addition to propene to be a relatively small source of propanone nitrate, at night it is often calculated to be the dominant source, which may explain some of the night-time peaks in propanone nitrate.¶
¶
The main source of the δ-IHN is modelled to come from OH addition to isoprene, but on certain nights the source from $NO_3$ addition to isoprene led to modelled mixing ratios of around 15-30 ppt of (4-OH, 1-$ONO_2$)-IHN coincident with enhanced modelled mixing ratios of the δ-ICN. We were unable to detect δ-IHN despite the modelled mixing ratios being considerably greater than our detection limit, nor did we detect strong enhancements in the mixing ratios of the δ-ICN, so again raises questions concerning our understanding of the $NO_3$ initiated isoprene degradation chemistry¶
¶
This study demonstrates the need for further measurements of speciated IN measurements to test our understanding of the isoprene degradation chemistry. Our interpretation is limited by the uncertainties in our measurements and relatively small data set, but highlights areas of the isoprene chemistry that warrant further study, in particular the impact of NO on the formation of the β-IHN, and the $NO_3$ initiated isoprene degradation chemistry.¶

measurements of other chemical species (e.g. other products of the nitrooxy-peroxy radicals), as well as improved quantification of several reaction rate constants. Further laboratory studies are required to improve quantification of the IN lifetimes, in particular with respect to photolysis of the ICN, deposition and hydrolysis, and to better constrain the peroxy radical reactions, including the branching ratio of the NO reaction that leads to IHN.

*Code Availability.* The MCM code is available from the authors on request.

*Data Availability*. The observational data and diel cycles from the MCM in the figures are in the Supplementary Information. The 15 minute data from the MCM is available from the authors on request.

*Supplement.*

*Author contributions.* CER led the data interpretation and writing of the manuscript. GPM made the measurements of the IN with the assistance of YL. LKW did the MCM modelling. CER, WJB, SG, DEH, CNH, RLJ, JDL, XW and CY were involved in the project planning and leading the measurement groups. WJA, LRC, JRH, SK, LJK, BO, ES, FS and RW-M provided measurement data. All commented on the manuscript.

*Competing interests.* The authors declare that they have no conflict of interest.

*Acknowledgements.* We are grateful for funding provided by the UK Natural Environment Research Council (NERC), UK Medical Research Council and the Natural Science Foundation of China (NSFC) under the framework of the Newton Innovation Fund (NERC grants NE/N006909/1, NE/N006895/1, NE/N006976/1 and NE/N00700X/1; NSFC grant 41571130031). ES and RW-M are grateful to the NERC SPHERES Doctoral Training Programme for funding PhD studentships. CER acknowledges Andrew Rickard (NCAS, University of York) for providing information on the MCM.

**References**

Bates, K. H., and Jacob, D. J., A new model mechanism for atmospheric oxidation of isoprene: global effects on oxidants, nitrogen oxides, organic products, and secondary organic aerosol, Atmos. Chem. Phys., 19, 9613–9640, https://doi.org/10.5194/acp-19-9613-2019, 2019.

Bew, S. P., Hiatt-Gipson, G. D., Mills, G. P., and Reeves, C. E.: Efficient syntheses of climate impacting isoprene nitrates and (1R,5S)-(-)-myrtenol nitrate, Beilstein J. Org. Chem., 12, 1081–1095, doi:10.3762/bjoc.12.103, 2016.

Emmerson, K. M., and Evans, M. J.: Comparison of tropospheric gas-phase chemistry schemes for use within global models, Atmos. Chem. Phys., 9, 1831-1845, 2009.

Fiore, A. M., Horowitz, L. W., Purves, D. W., Levy II, H., Evans, M. J., Wang, Y., Li, Q., and Yantosca, R. M.: Evaluating the contribution of changes in isoprene emissions to surface ozone trends over the eastern United States, J. Geophys. Res., 110, D12303, doi: 10.1029/2004JD005485, 2005.

Guenther, A., Jiang, X., Heald, C. L., Sakulyanontvittaya, T., Duhl, T., Emmons, L. K., and Wang, X.: The Model of Emissions of Gases and Aerosols from Nature version 2.1 (MEGAN 2.1): An Extended and Updated Framework for Modeling Biogenic Emissions. Geosci. Model Dev., 5, 1471−1492, 2012.



**Moved down [12]:** R.,
**Deleted:** Beaver, M.
**Moved down [15]:** E.,
**Moved down [13]:** F.,
**Moved down [14]:** . W.,
**Moved down [16]:** J.,
**Moved down [17]:** Chem. Phys
**Deleted:** St Clair, J. M., Paulot,
**Deleted:** Spencer, K. M., Crounse, J. D., LaFranchi, B
**Deleted:** Min, K. E., Pusede, S.
**Deleted:** Wooldridge, P.
**Deleted:** Schade, G. W., Park, C., Cohen, R. C., and Wennberg, P. O.: Importance of biogenic precursors to the budget of organic nitrates: observations of multifunctional organic nitrates by CIMS and TD-LIF during BEARPEX 2009, Atmos. …
**Deleted:** ., 12, 5773-5785, doi: 10.5194/acp-12-5773-2012, 2012.¶
**Deleted:** Bohn, B
**Moved down [18]:** ., Heard, D.
**Deleted:** E., Mihalopoulos,
**Moved down [19]:** N.,
**Deleted:** Plass-Dülmer,
**Moved down [20]:** C.,
**Deleted:** Schmitt, R., and
**Moved down [21]:** Whalley, L.
**Deleted:** K.: Characterisation and improvement of $j(O^1D)$ filter radiometers, Atmos. Meas. Tech., 9, 3455– 3466, …
**Moved down [22]:** A.,
**Deleted:** Flocke, F., McKeen, S. A., Brioude, J., Sommariva,
**Moved down [23]:** R.,
**Deleted:** Trainer, Fehsenfeld, F. C., and Ravishankara, A. R.: …
**Moved down [24]:** D.,
**Deleted:** and Shepson, P. B.: Measurement of the organic nitrate …
**Moved down [25]:** R., Kramer, L
**Deleted:** ., Pope, F. D.,
**Moved down [26]:** Whalley, L.
**Deleted:** K., Cryer, D. R., Heard, D. E., Lee, J.
**Moved down [27]:** D.,
**Deleted:** Reed, C., and Bloss, W. J.: On the interpretation of in s …
**Moved down [28]:** . Discuss.,
**Deleted:** 189, 191–212, 2016.¶ …
**Deleted:** Fisher, J. A., Jacob, D
**Moved down [29]:** . J.,
**Deleted:** Travis, K. R., Kim, P. S., Marais, E. A., Chan Miller, C …
**Moved down [30]:** L.,
**Deleted:** Yantosca, R. M., Sulprizio, M. P., Mao
**Moved down [31]:** J.,
**Deleted:** Wennberg, P. O., Crounse,
**Moved down [32]:** J.
**Deleted:** D., Teng, A. P., Nguyen, T. B., St. Clair, J. M., Cohen, …
**Moved down [33]:** F.,
**Deleted:** Blake, D. R., Goldstein, A. H., Misztal, P. K., Hanisco …

Hamilton, J. F., Bryant, D. J., Edwards, P. E., Ouyang, B., Bannan, T. J., Mehra, A., Mayhew, A. W., Hopkins, J. R., Dunmore, R. E., Squires, F. A., Lee, J. D., Newland, M. J., Worrall, S. D., Bacak, A., Coe, H., Percival, C., Whalley, L. K., Heard, D. E., Slater, E. J., Jones, R. J., Cui, T., Surratt, J. D., Reeves, C. E., Mills, G. P., Grimmond, S., Sun, Y., Xu, W., Shi, Z., Rickard, A. R.: Key Role of NO3 Radicals in the Production of Isoprene Nitrates and Nitrooxyorganosulfates in Beijing, accepted in Environ Sci Technol, doi: 10.1021/acs.est.0c05689, 2021.

Jacobs, M. I., Burke, W. J., and Elrod, M. J.: Kinetics of the reactions of isoprene-derived hydroxynitrates: gas phase epoxide formation and solution phase hydrolysis, Atmos. Chem. Phys., 14, 8933-8946, doi: 10.5194/acp-14-8933-2014, 2014.

Jenkin, M. E., Young, J. C., and Rickard, A. R.: The MCM v3.3.1 degradation scheme for isoprene, Atmos. Chem. Phys., 15, 11433-11459, doi: 10.5194/acp-15-11433-2015, 2015.

Lee, L., Teng, A. P., Wennberg, P. O., Crounse, J. D., and Cohen, R. C.: On Rates and Mechanisms of OH and $O_3$ Reactions with Isoprene Derived Hydroxy Nitrates, J. Phys. Chem., 118, 1622-1637, doi: 10.1021/jp4107603, 2014.

Lockwood, A. L., Shepson, P. B., Fiddler, M. N., and Alaghmand, M.: Isoprene nitrates: preparation, separation, identification, yields, and atmospheric chemistry, Atmos. Chem. Phys., 10, 6169-6178, doi: 10.5194/acp-10-6169-2010, 2010.

Mills, G. P., Hiatt-Gipson, G. D., Bew, S. P., and Reeves, C. E.: Measurement of isoprene nitrates by GCMS, Atmos. Meas. Tech., 9, 4533-4545, doi: 10.5194/amt-9-4533-2016, 2016.

Müller, J.-F., Peeters, J., and Stavrakou, T.: Fast photolysis of carbonyl nitrates from isoprene, Atmos. Chem. Phys., 14, 2497-2508, doi: 10.5194/acp-14-2497-2014, 2014.

Newland, M. J., Bryant, D. J., Dunmore, R. E., Bannan, T. J., Acton, W. J. F., Langford, B., Hopkins, J. R., Squires, F. A., Dixon, W., Drysdale, W. S., Ivatt, P. D., Evans, M. J., Edwards, P. M., Whalley, L. K., Heard, D. E., Slater, E. J., Woodward-Massey, R., Ye, C., Mehra, A., Worrall, S. D., Bacak, A., Coe, H., Percival, C. J., Hewitt. C. N., Lee, J. D., Cui, T., Surratt, J. D., Wang, X., Lewis, A. C., Rickard. A. R., Hamilton, J. F., Rainforest-like Atmospheric Chemistry in a Polluted Megacity, Atmos. Chem, Phys., under review, https://doi.org/10.5194/acp-2020-35, 2020.

Nguyen, T. B., Crounse, J. D., Schwantes, R. H., Teng, A. P., Bates, K. H., Zhang, X., St. Clair, J. M., Brune, W. H., Tyndall, G. S., Keutsch, F. N., Seinfeld, J. H., and Wennberg, P. O.: Overview of the Focused Isoprene eXperiment at the California Institute of Technology (FIXCIT): mechanistic chamber studies on the oxidation of biogenic compounds, Atmos. Chem. Phys., 14, 13531-13549, doi: 10.5194/acp-14-13531-2014, 2014.

Nguyen, T. B., Crounse, J. D., Teng, A. P., St Clair, J. M., Paulot, F., Wolfe, G. M., and Wennberg, P. O.: Rapid deposition of oxidized biogenic compounds to a temperate forest, P. Natl. Acad. Sci., 112, E392-E401, doi: 10.1073/pnas.1418702112, 2015.

Peeters, J., Nguyen, T. L., and Vereecken, L.: HOx radical regeneration in the oxidation of isoprene, Phys. Chem. Chem. Phys., 28, 5935–5939, 2009.

Saunders, S. M., Jenkin, M. E., Derwent, R. G., and Pilling, M. J.: Protocol for the development of the Master Chemical Mechanism, MCM v3 (Part A): tropospheric degradation of non-aromatic volatile organic compounds, Atmos. Chem. Phys., 3, 161-180, 2003.



**Moved (insertion) [13]**

**Moved (insertion) [34]**

**Moved (insertion) [16]**

**Moved (insertion) [14]**

**Moved (insertion) [12]**

**Moved (insertion) [22]**

**Moved (insertion) [24]**

**Moved (insertion) [21]**

**Moved (insertion) [18]**

**Moved (insertion) [35]**

**Deleted:** Horowitz, L. W., Fiore, G. P., Milly, A. M., Cohen, R. C., Perring, A., Wooldridge, P. J., Hess, P. G., Emmons, L. K., and Lamarque, J.: Observational constraints on the chemistry of isoprene nitrates over the eastern United States, J. Geophys. Res., 112, D12S08, doi:10.1029/2006JD007747, 2007.¶

**Deleted:** Kennedy, O. J.,

**Moved down [36]:** Ouyang, B.,

**Deleted:** Langridge, J. M., Daniels, M. J. S., Bauguitte, S., Freshwater, R., McLeod, M. W., Ironmonger, C., Sendall, J., Norris, O., Nightingale, R., Ball, S. M., and…

**Moved up [35]:** Jones, R.

**Deleted:** L.: An aircraft based three channel broadband cavity enhanced absorption spectrometer for simultaneous measurements of $NO_3$, $N_2O_5$ and $NO_2$, Atmos. Meas. Tech., 4, 9, 1759-1776, DOI: 10.5194/amt-4-1759-2011, 2011. ¶
Kotthaus, S. and Grimmond, C. S. B.: Atmospheric boundary layer characteristics from ceilometer measurements part 1: A new method to track mixed layer height and classify clouds, Q. J. Roy. Meteorol. Soc., 144, 1525–1538, https://doi.org/10.1002/qj.3299, 2018.¶
Kwan, A. J., Chan, A. W. H., Ng, N. L., Kjaergaard, H. G., Seinfeld, J. H., and Wennberg, P. O.: Peroxy Radical Chemistry and OH Radical Production during the NO3-Initiated Oxidation of Isoprene, Atmos. Chem. Phys., 12, 7499−7515, 2012.¶

**Deleted:** Lee, B. H., Lopez-Hilfiker, F. D., D'Ambro, E. L., Zhou, P., Boy, M., Petäjä, T., Hao, L., Virtanen, A., and Thornton, J. A.: Semi-volatile and highly oxygenated gaseous and particulate organic compounds observed above a boreal forest canopy, Atmos. Chem. Phys., 18, 11547-11562, doi: 10.5194/acp-18-11547-2018, 2018. ¶
Li, R., Jiang, X.,

**Moved down [37]:** Wang, X.,

**Deleted:** Chen, T., Du, L., Xue, L., Bi, X,. Tang, M., and Wang, W., Determination of Semivolatile Organic Nitrates in Ambient Atmosphere by Gas Chromatography/Electron Ionization–Mass Spectrometry, Atmosphere, 10, 88, doi:10.3390/atmos10020088, 2019.¶

**Deleted:** Mao, J., Paulot, F., Jacob, D. J., Cohen, R. C., Crounse, J. D., Wennberg, P. O., Keller, C. A., Hudman, R. C., Barkley, M. P., and Horowitz, L. W.: Ozone and organic nitrates over the eastern United States: Sensitivity to isoprene chemistry, J. Geophys. Res.: Atmospheres, 118, 11,256-11,268, doi: 10.1002/jgrd.50817, 2013.¶

**Deleted:** Paulot, F., Crounse, J. D., Kjaergaard, H. G., Kroll, J. H., Seinfeld, J. H., and Wennberg, P. O.: Isoprene photooxidation: new insights into the production of acids and organic nitrates, Atmos. Chem. Phys., 9, 1479-1501, 2009.¶
Paulot, F., Henze, D. K., and Wennberg, P. O.: Impact of the isoprene photochemical cascade on tropical ozone, Atmos. Chem. Phys., 12, 1307-1325, doi: 10.5194/acp-12-1307-2012, 2012.¶

**Deleted:** Perring, A.E., Bertram, T.H., Wooldridge, P.J., Fried, A., Heikes, B.G., Dibb, J., Crounse, J.D., Wennberg, P.O., Blake, N.J., Blake, D.R., Brune, W.H., Singh, H.B., and Cohen, R.C, Airborne observations of total $RONO_2$: new constraints on the yield and lifetime of isoprene nitrates., Atmos. Chem. Phys., 9 (4), 1451-1463, 2009a.¶
Perring, A. E., Wisthaler, A., Graus, M., Wooldridge, P. J., Lockwood, A. L., Mielke, L. H., Shepson, P. B., Hansel, A., and Cohen, R. C.,

Schwantes, R. H., Teng, A. P., Nguyen, T. B., Coggon, M. M., Crounse, J. D., St Clair, J. M., Zhang, X., Schilling, K. A., Seinfeld, J. H. and Wennberg, P. O.: Isoprene $NO_3$ Oxidation Products from the $RO_2$ + $HO_2$ Pathway, J. Phys. Chem., 119, 10158-10171, doi: 10.1021/acs.jpca.5b06355, 2015.

Schwantes, R. H., Emmons, L. K., Orlando, J. J., Barth, M. C., Tyndall, G. S., Hall, S. R., Ullmann, K., St. Clair, J. M., Blake, D. R., Wisthaler, A., and Bui, T. P. V., Comprehensive isoprene and terpene gas-phase chemistry improves simulated surface ozone in the southeastern US, Atmos. Chem. Phys., 20, 3739–3776, https://doi.org/10.5194/acp-20-3739-2020, 2020.

Shi, Z., Vu, T., Kotthaus, S., Harrison, R. M., Grimmond, S., Yue, S., Zhu,T., Lee,J., Han,Y., Demuzere,M., Dunmore,R.E., Ren, L., Liu,D., Wang,Y., Wild,O., Allan,J., Acton,W.J., Barlow,J., Barratt, B., Beddows, D., Bloss, W. J., Calzolai, G., Carruthers, D., Carslaw, D. C., Chan, Q., Chatzidiakou, L., Chen, Y., Crilley, L., Coe, H., Dai, T., Doherty, R., Duan, F., Fu, P., Ge, B., Ge, M., Guan, D., Hamilton, J. F., He, K., Heal, M., Heard, D., Hewitt, C. N., Hollaway, M., Hu, M., Ji, D., Jiang, X., Jones, R., Kalberer, M., Kelly, F. J., Kramer, L., Langford, B., Lin, C., Lewis, A. C., Li, J., Li, W., Liu, H., Liu, J., Loh, M., Lu, K., Lucarelli, F., Mann, G., McFiggans, G., Miller, M. R., Mills, G., Monk, P., Nemitz, E., O'Connor, F., Ouyang, B., Palmer, P. I., Percival, C., Popoola, O., Reeves, C., Rickard, A. R., Shao, L., Shi, G., Spracklen, D., Stevenson, D., Sun, Y., Sun, Z., Tao, S., Tong, S., Wang, Q., Wang, W., Wang, X., Wang, X., Wang, Z., Wei, L., Whalley, L., Wu, X., Wu, Z., Xie, P., Yang, F., Zhang, Q.,Zhang, Y.,Zhang,Y., and Zheng, M.: Introduction to the special issue "In-depth study of air pollution sources and processes within Beijing and its surrounding region (APHH-Beijing)", Atmos. Chem. Phys., 19, 7519–7546, https://doi.org/10.5194/acp19-7519-2019, 2019.

Squire, O. J., Archibald, A. T., Griffiths, P. T., Jenkin, M. E., Smith, D., and Pyle, J. A: Influence of isoprene chemical mechanism on modelled changes in tropospheric ozone due to climate and land use over the 21st century, Atmos. Chem. Phys., 15, 5123-5143, doi: 10.5194/acp-15-5123-2015, 2015.

Teng, A. P., Crounse, J. D., and Wennberg, P. O.: Isoprene Peroxy Radical Dynamics, J. Am. Che. Soc., 139, 5367-5377, doi: 10.121/jacs.6b12838, 2017.

Vasquez, K. T., Allen, H. M., Crounse, J. D., Praske, E., Xu, L., Noelscher, A. C., and Wennberg, P. O.: Low-pressure gas chromatography with chemical ionization mass spectrometry for quantification of multifunctional organic compounds in the atmosphere, Atmos. Meas. Tech., 11, 6815-6832, doi: 10.5194/amt-11-6815-2018, 2018.

Von Kuhlmann, R., Lawrence, M. G., Pöschl, U., and Crutzen, P. J.: Sensitivities in global scale modeling of isoprene, Atmos. Chem. Phys., 4, 1-17, 2004.

Wennberg, P. O., Bates, K. H., Crounse, J. D., Dodson, L. G., McVay, R. C., Mertens, L. A., Nguyen, T. B., Praske, E., Schwantes, R. H., Smarte, M. D., St Clair, J. M., Teng, A. P., Zhang, X., and Seinfeld, J. H.: Gas-Phase Reactions of Isoprene and Its Major Oxidation Products, Chem. Rev., 118, 3337-3390, doi: 10.1021/acs.chemrev.7b00439, 2018.

Whalley, L. K., Slater, E. J., Woodward-Massey, R., Ye, C., Lee, J. D., Squires, F., Hopkins, J. R., Dunmore, R. E., Shaw, M., Hamilton, J. F., Lewis, A. C., Mehra, A., Worrall, S. D., Bacak, A., Bannan, T. J., Coe, H., Ouyang, B., Jones, R. L., Crilley, L. R., Kramer, L. J., Bloss, W. J., Vu, T., Kotthaus, S., Grimmond, S., Sun, Y., Xu, W., Yue, S., Ren, L., Acton, W. J. F., Hewitt, C. N., Wang, X., Fu, P., and Heard, D. E.: Evaluating the sensitivity of radical chemistry and ozone formation to ambient VOCs and NOx in Beijing, Atmos. Chem. Phys. Discuss., https://doi.org/10.5194/acp-2020-785, in review, 2020.

**Moved up [34]:** ., Edwards, P.

**Deleted:** Smith, K. R

**Moved down [38]:** Lewis, A.

**Deleted:** M., Evans, M. J., Lee, J. D., Shaw, M. D., Squires, F., Wilde, S., and Lewis, A. C.: Clustering approaches to improve the

**Deleted:** C.: Clustering approaches to improve the performance of low cost air pollution sensors, Faraday Discuss., 200, 321–637, https://doi.org/10.1039/C7FD00020K, 2017.¶

**Deleted:** Werner, G., Kastler, J ., Looser, R., and Ballschmiter, K., Organic nitrates of isoprene as atmospheric trace compounds, Angewandte Chemie-Int. Ed., 38(11), 1634-1637. 1999. DOI: 10.1002/(SICI)1521-3773(19990601)38:11¶

**Moved (insertion) [26]**

**Moved (insertion) [23]**

**Moved (insertion) [15]**

**Moved (insertion) [38]**

**Moved (insertion) [20]**

**Moved (insertion) [27]**

**Moved (insertion) [36]**

**Moved (insertion) [30]**

**Moved (insertion) [25]**

**Moved (insertion) [29]**

**Moved (insertion) [31]**

**Moved (insertion) [32]**

**Moved (insertion) [33]**

**Moved (insertion) [19]**

**Moved (insertion) [37]**

**Moved (insertion) [17]**

**Moved (insertion) [28]**

Wu, S., Mickley, L. J., Jacob, D. J., Logan, J. A. Yantosca, R. M., and Rind, D.: Why are there large differences between models in global budgets of tropospheric ozone?, J. Geophys. Res., 112, D5, D05302, doi: 10.1029/2006JD007801, 2007.

Xiong, F., McAvey, K. M., Pratt, K. A., Groff, C. J., Hostetler, M. A., Lipton, M. A., Starn, T. K., Seeley, J. V., Bertman, S. B., Teng, A. P., Crounse, J. D., Nguyen, T. B., Wennberg, P. O., Misztal, P. K., Goldstein, A. H., Guenther, A. B., Koss, A. R., Olson,K. F., de Gouw, J. A., Baumann, K., Edgerton, E. S., Feiner, P. A., Zhang, L., Miller, D. O., Brune, W. H., and Shepson, P. B.: Observation of isoprene hydroxynitrates in the southeastern United States and implications for the fate of NOx, Atmos. Chem. Phys., 15, 11257-11272, doi: 10.5194/acp-15-11257-2015, 2015.

Xiong, F., Borca, C. H., Slipchenko, L. V., and Shepson, P. B.: Photochemical degradation of isoprene-derived 4,1-nitrooxy enal, Atmos. Chem. Phys., 16, 5595-5610, doi: 10.5194/acp-16-5595-2016, 2016.

**Deleted:** Xie, Y., Paulot, F., Carter, W. P. L., Nolte, C. G., Luecken, D. J., Hutzell, W. T., Wennberg, P. O., Cohen, R. C., and Pinder, R. W.: Understanding the impact of recent advances in isoprene photooxidation on simulations of regional air quality, Atmos. Chem. Phys., 13, 8439-8455, doi: doi:10.5194/acp-13-8439-2013, 2013.¶

**Deleted:** ¶
Zare, A., Romer, P. S., Nguyen, T., Keutsch, F. N., Skog, K., and Cohen, R. C.: A comprehensive organic nitrate chemistry: insights into the life time of atmospheric organic nitrates, Atmos. Chem. Phys., 15, 15419-15436, doi: 10.5194/acp-18-15419-2018, 2018. ¶

**Table 1: Uncertainties in the measurements of the isoprene nitrates**

| Isoprene nitrate | Period 1 (metal valve, column and trap) | Period 2 (plastic valve and direct injection) | Period 3 (plastic valve, column and trap) |
|---|---|---|---|
| (4-OH, 3-$ONO_2$)-IHN | 15% + 0.1 ppt | 14% + 1 ppt | 14% +0.1 ppt |
| (1-OH, 2-$ONO_2$)-IHN | - | 22% + 1 ppt | - |
| E-(1-OH, 4-$ONO_2$)-ICN | 27% + 0.1 ppt | - | 22% +0.1 ppt |
| E-(4-OH, 1-$ONO_2$)-ICN | 24% + 0.1 ppt | - | 22% +0.1 ppt |
| Z-(1-OH, 4-$ONO_2$)-ICN | 23% + 0.1 ppt | - | 22% +0.1 ppt |
| Z-(4-OH, 1-$ONO_2$)-ICN | 24% + 0.1 ppt | - | 22% +0.1 ppt |
| Propanone nitrate | 18% + 0.1 ppt | - | 17% +0.1 ppt |

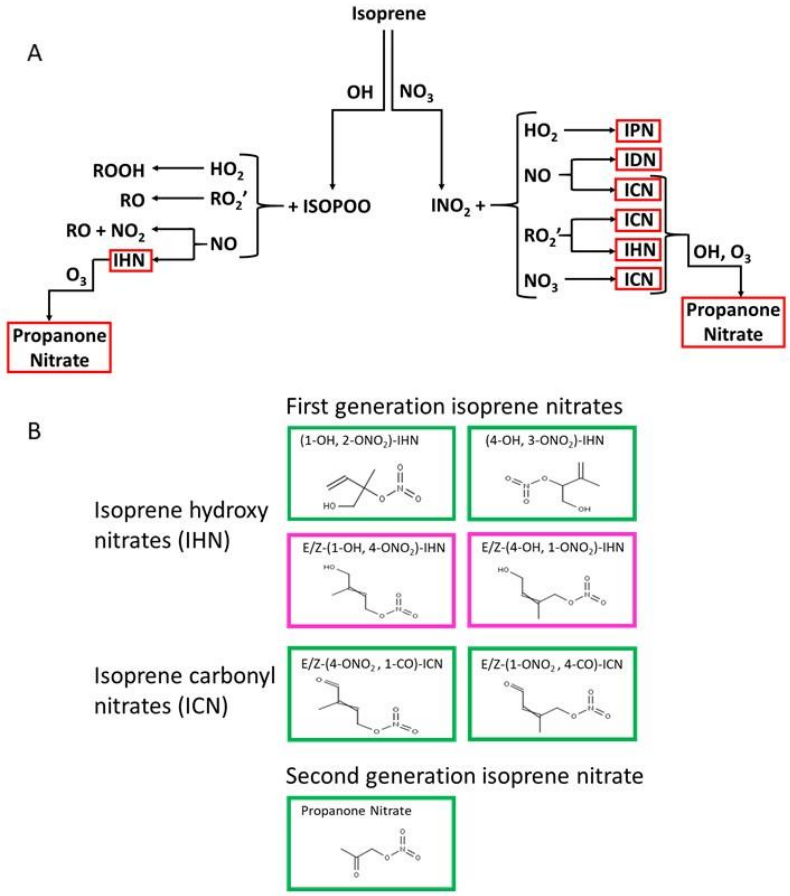


**Figure 1: A) Formation of IN (red boxes) from isoprene oxidation by OH and $NO_3$: isoprene hydroxy nitrates (IHN): isoprene hydroperoxy nitrates (IPN); isoprene dinitrates (IDN); isoprene carbonyl nitrates (ICN); and propanone nitrate. B) The skeletal formula of the specific IN discussed in this paper. Box colours: Green - measured in Beijing; Pink - measured by the analytical system previously in the laboratory, but not discernible in Beijing.**

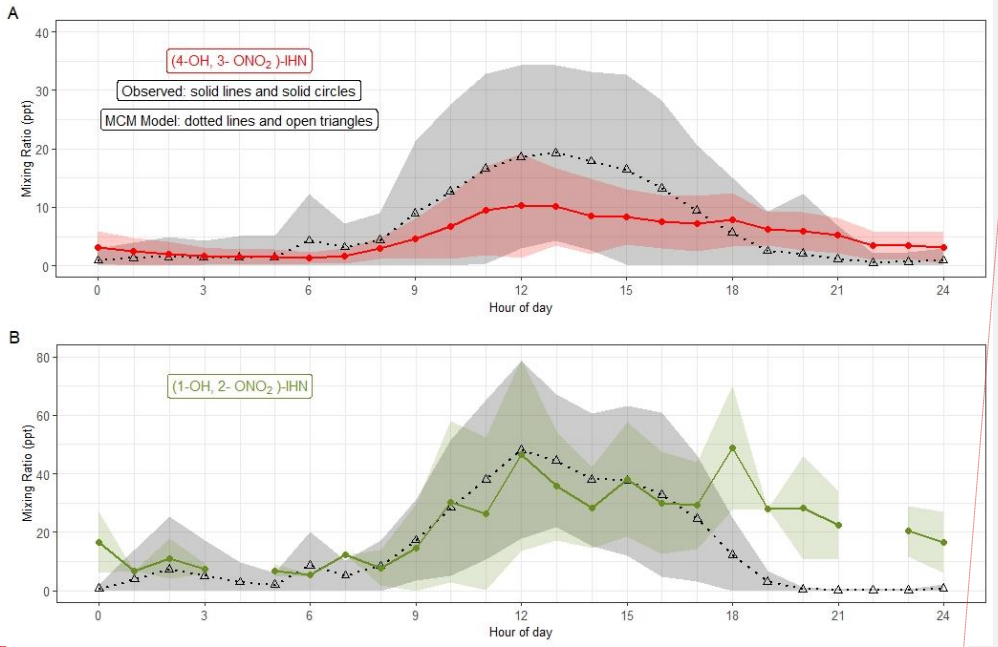


**Figure 2: Modelled and observed mixing ratios of (a) (4-OH, 3-$ONO_2$)-IHN and (b) (1-OH, 2-$ONO_2$)-IHN. Data points are the means and the shaded areas represent ±1 s.d. in the variability of values for each hour of the day.**

Deleted: ¶
¶

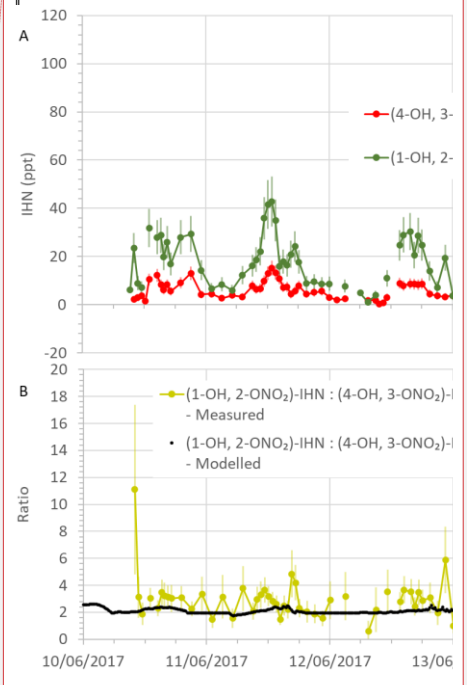


**Figure 2**

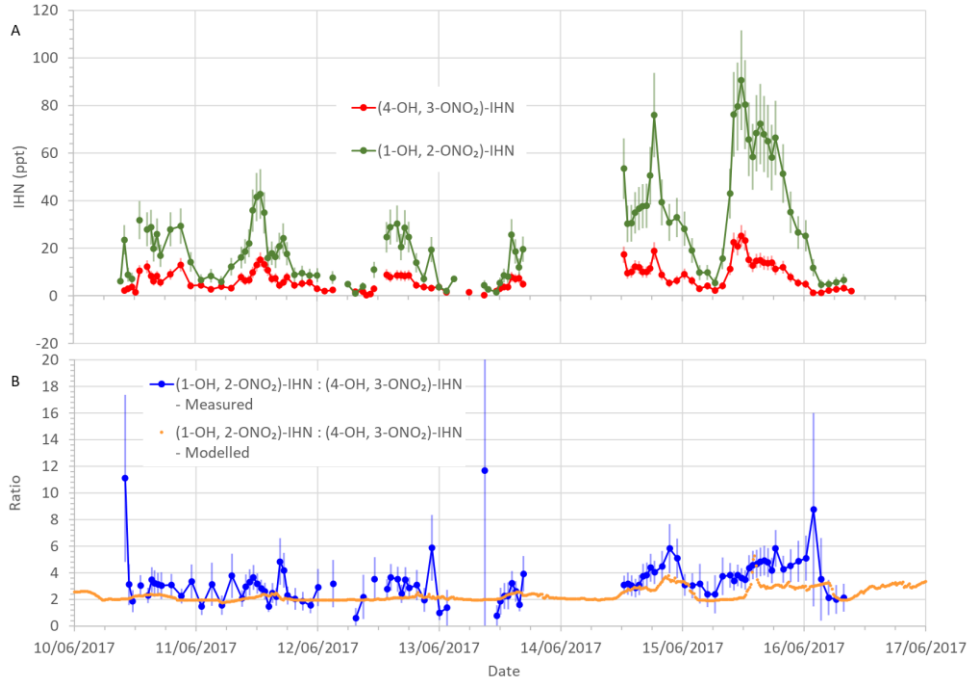


**Figure 3: a) Measured β-IHN mixing ratios. b) Measured and modelled ratio (1-OH, 2-ONO₂)-IHN:(4-OH, 3-ONO₂)-IHN. Error bars are the measurement uncertainties (see Sect. 3.3 for details).**

**Deleted:**

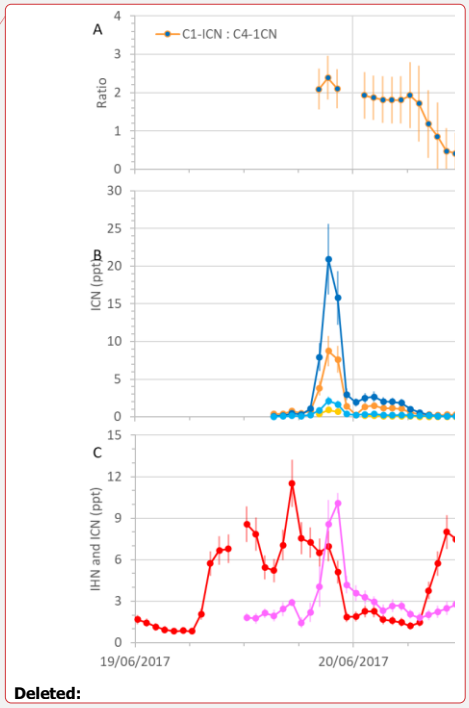

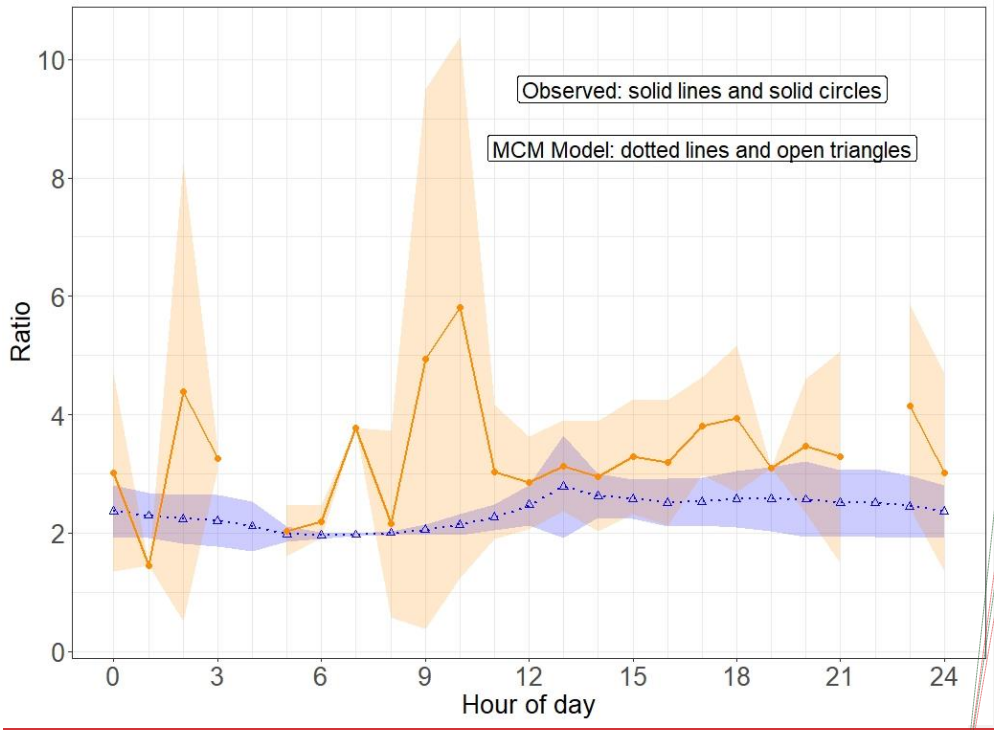


**Figure 4: Modelled and observed (1-OH, 2-$ONO_2$)-IHN / (4-OH, 3-$ONO_2$)-IHN ratio. Data points are the means and the shaded areas represent ±1 s.d. in the variability of values for each hour of the day.**

**Moved down [39]: : Measured δ-ICN mixing ratios and ratios of C1-ICN to C4-ICN, along with (4-OH, 3-$ONO_2$)-IHN and propanone nitrate mixing ratios during the last four days of the summer campaign. Error bars are the measurement uncertainties (see Sect. 3.3 for details).¶**

**Deleted: 3**

**Moved down [40]: ¶**
**Figure 5**

**Deleted: ¶**

Page Break

¶
¶

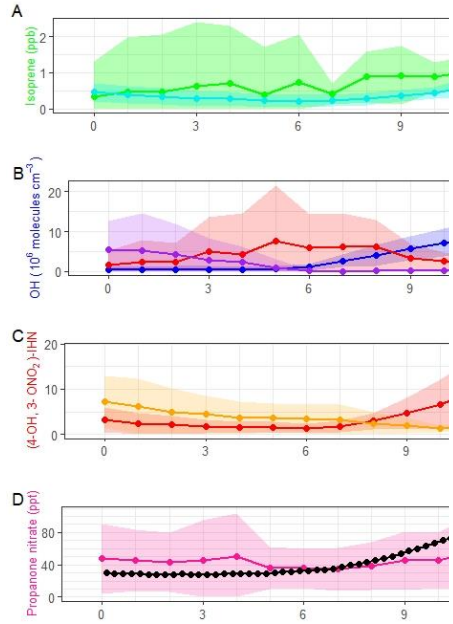


**Figure 4: Diel patterns of trace gases derived from the measured mixing ratios for each hour of the day. Data points for the mixing ratios are the means and the shaded areas represent ±1 s.d. in the variability of values for each hour of the day. Also shown are the means of the mixed layer height for each 15 minute period of the day.¶**

Page Break

¶
¶

**Deleted: mixing ratios of (a)**

**Deleted: and (b) (1-OH, 2-$ONO_2$)-IHN**

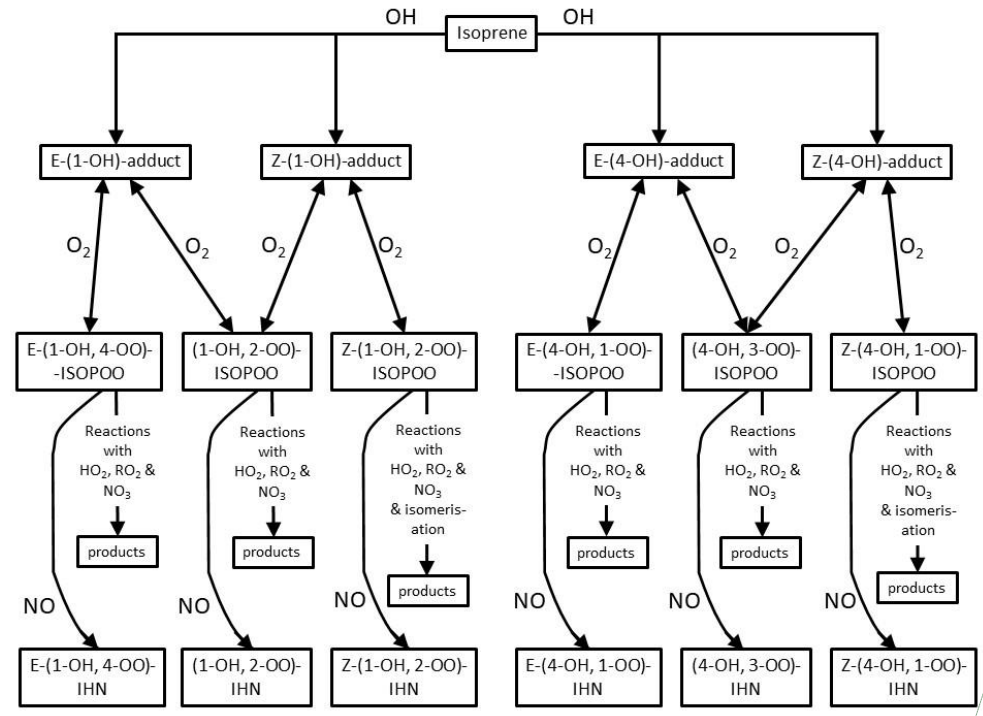


**Figure 5: Schematic of the formation of the IHN following addition of OH to the C1 and C4 positions.**

**Moved (insertion) [40]**

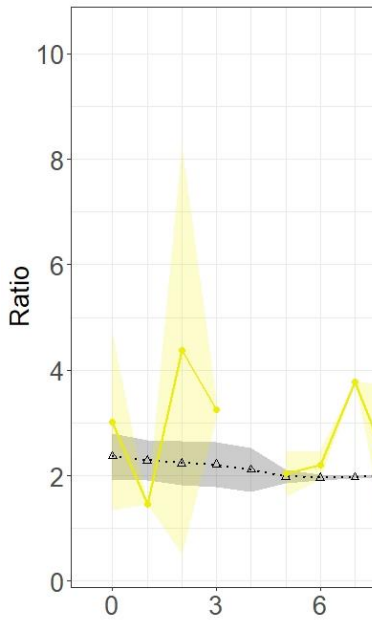


**Deleted:**
¶
**Figure 6: Modelled and observed (1-OH, 2-$ONO_2$)-IHN / (4-OH, 3-$ONO_2$)-IHN ratio. Data points are the means and the shaded areas represent ±1 s.d. in the variability of values for each hour of the day.**

Page Break

¶
¶

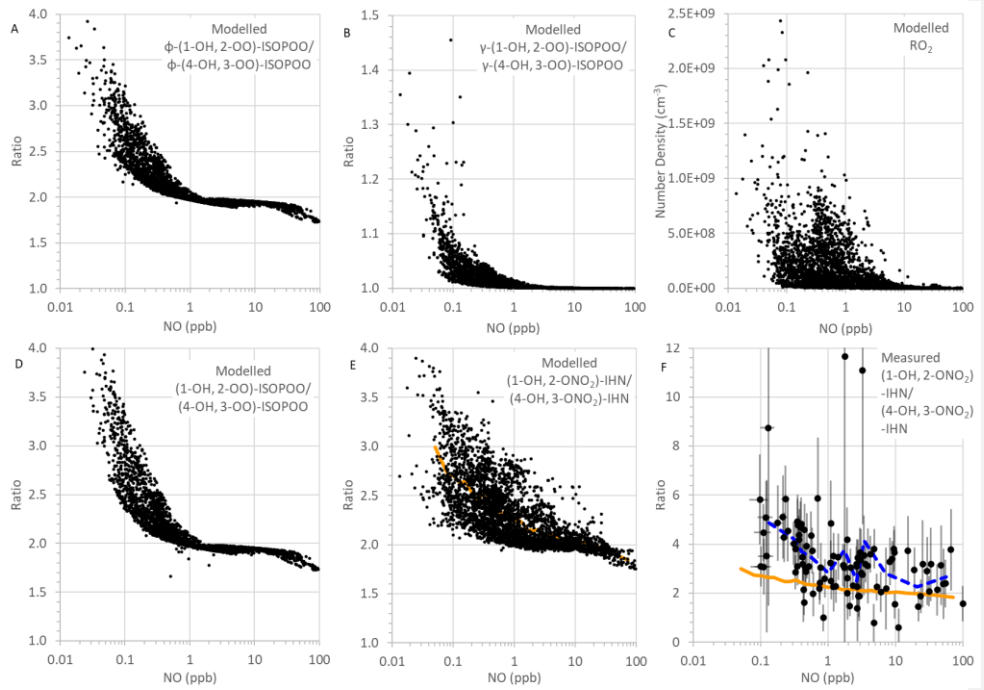


**Figure 6: MCM modelled and measured parameters as a function of NO mixing ratio: (a) Modelled ratio of φ-(1-OH, 2-OO)-ISOPOO to φ- (4-OH, 3-OO)-ISOPOO; (b) Modelled ratio of γ-(1-OH, 2-OO)-ISOPOO to γ-(4-OH, 3-OO)-ISOPOO; (c) Modelled $RO_2$ number density; (d) Modelled ratio of (1-OH, 2-OO)-ISOPOO to (4-OH, 3-OO)-ISOPOO; (e) Modelled ratio of (1-OH, 2-$ONO_2$)-IHN to (4-OH, 3-$ONO_2$)-IHN; (f) Measured ratio of (1-OH, 2-$ONO_2$)-IHN to (4-OH, 3-$ONO_2$)-IHN (error bars are the measurement uncertainties (see Sect. 3.3 for details)). In panel E the orange line is a trend line produced by plotting the mean modelled (1-OH, 2-$ONO_2$)-IHN to (4-OH, 3-$ONO_2$)-IHN ratio for each bin of one hundred NO mixing ratios. This same line is plotted in panel F for comparison with the observed data. The blue dashed line in panel F is a trend line produced by plotting the mean measured (1-OH, 2-$ONO_2$)-IHN to (4-OH, 3-$ONO_2$)-IHN ratio for each bin of nine NO mixing ratios.**

**Deleted:** 3.3 for details)).

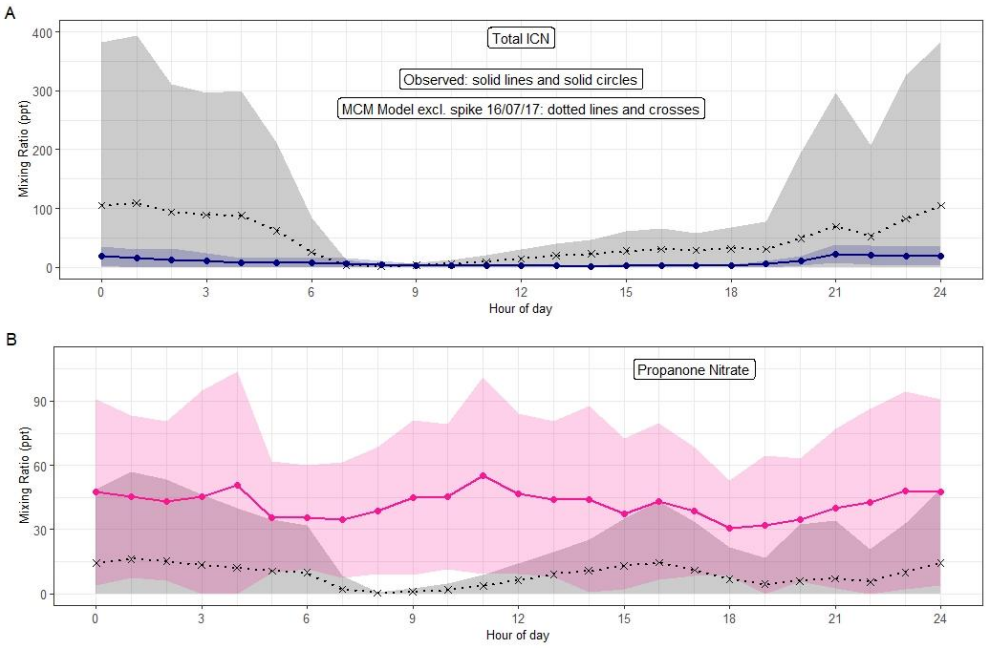


**Figure 7: (a) Diel pattern of total ICN as modelled using the MCM and measured. For the MCM this is the specie NC4CHO, whilst the measurements are the sum of the four δ-ICN (E and Z-(1-$ONO_2$, 4-CO)-ICN and E and Z-(4-$ONO_2$, 1-CO)-ICN). (b) Diel pattern of propanone as modelled using the MCM and measured. Data points are the means and the shaded areas represent ±1 s.d. in the variability of values for each hour of the day.**

Deleted: 8

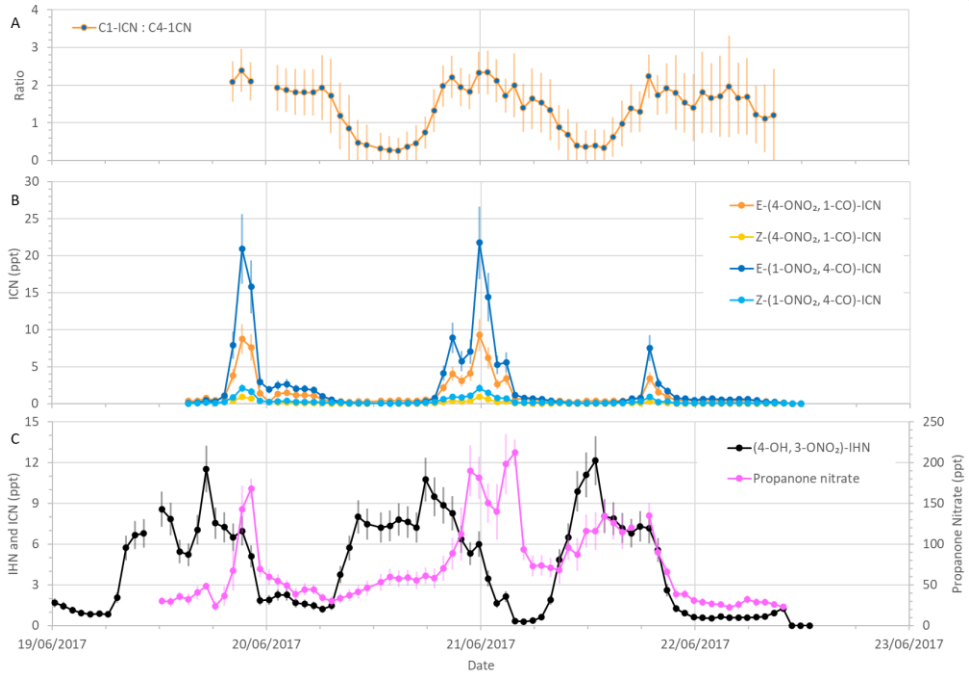


**Figure 8: Measured δ-ICN mixing ratios and ratios of C1-ICN to C4-ICN, along with (4-OH, 3-$ONO_2$)-IHN and propanone nitrate mixing ratios during the last four days of the summer campaign. Error bars are the measurement uncertainties (see Sect. 3.3 for details). The vertical grid lines indicate midnight on each day.**

Moved (insertion) [39]

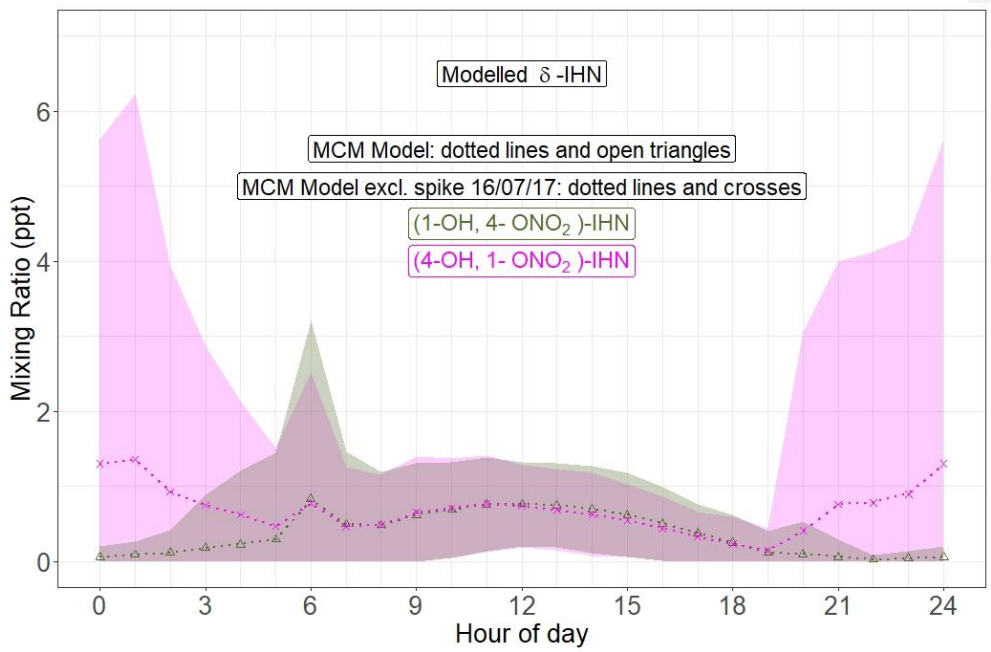


**Figure 9: Diel pattern of MCM modelled δ-IHN ((1-OH, 4-$ONO_2$)-IHN and (4-OH, 1-$ONO_2$)-IHN). Data points are the means and the shaded areas represent ±1 s.d. in the variability of values for each hour of the day.**